Molecular Biology of the Cell
Vol. 17, 3031–3050, July 2006

Amino Acids Regulate Retrieval of the Yeast General Amino Acid Permease from the Vacuolar Targeting Pathway

Marta Rubio-Texeira and Chris A. Kaiser

Department of Biology, Massachusetts Institute of Technology, Cambridge, MA 02139

Submitted July 25, 2005; Revised April 10, 2006; Accepted April 14, 2006
Monitoring Editor: Howard Riezman

Intracellular sorting of the general amino acid permease (Gap1p) in *Saccharomyces cerevisiae* depends on availability of amino acids such that at low amino acid concentrations Gap1p is sorted to the plasma membrane, whereas at high concentrations Gap1p is sorted to the vacuole. In a genome-wide screen for mutations that affect Gap1p sorting we identified deletions in a subset of components of the ESCRT (endosomal sorting complex required for transport) complex, which is required for formation of the multivesicular endosome (MVE). Gap1p-GFP is delivered to the vacuolar interior by the MVE pathway in wild-type cells, but when formation of the MVE is blocked by mutation, Gap1p-GFP efficiently cycles from this compartment to the plasma membrane, resulting in unusually high permease activity at the cell surface. Importantly, cycling of Gap1p-GFP to the plasma membrane is blocked by high amino acid concentrations, defining recycling from the endosome as a major step in Gap1p trafficking under physiological control. Mutations in *LST4* and *LST7* genes, previously identified for their role in Gap1p sorting, similarly block MVE to plasma membrane trafficking of Gap1p. However, mutations in other recycling complexes such as the retromer had no significant effect on the intracellular sorting of Gap1p, suggesting that Gap1p follows a genetically distinct pathway for recycling. We previously found that Gap1p sorting from the Golgi to the endosome requires ubiquitination of Gap1p by an Rsp5p ubiquitin ligase complex, but amino acid abundance does not appear to significantly alter the accumulation of polyubiquitinated Gap1p. Thus the role of ubiquitination appears to be a signal for delivery of Gap1p to the MVE, whereas amino acid abundance appears to control the cycling of Gap1p from the MVE to the plasma membrane.

INTRODUCTION

The family of amino acid permeases expressed in *Saccharomyces cerevisiae* fall into two different classes with respect to their regulation. Most of the permeases are expressed constitutively and import specific amino acids or chemically related amino acids. A second class of permeases are most highly expressed under conditions of nitrogen limitation and are thought to scavenge amino acids for their use as a source of nitrogen (Magasanik and Kaiser, 2002). The major nitrogen-scavenging permeases are Gap1p, which transports all naturally occurring amino acids with a high capacity (Grenson *et al.*, 1970; Jauniaux and Grenson, 1990), and Put4p, which is specific for proline (Vandenbol *et al.*, 1989). In part, the activity of Gap1p and Put4p is determined by an intracellular sorting decision, which depends on the nitrogen source in the growth medium. When yeast cells are grown on medium that lacks amino acids, Gap1p and Put4p are delivered to the plasma membrane where they are active for amino acid uptake. However, when cells are grown on a medium rich in an amino acid such as glutamate, Gap1p and Put4p are sorted to the vacuole for degradation (Roberg *et al.*, 1997a; Chen and Kaiser, 2002).

Mutations that affect the intracellular sorting of Gap1p can be classified into two general types. The first type includes mutations that cause constitutive sorting of high levels of Gap1p to the plasma membrane. This category includes in the genes *RSP5*, *BUL1*, *BUL2*, and *DOA4*, all of which either partially or completely block the intracellular ubiquitination of Gap1p, which serves as a tag for sorting to the vacuole (Helliwell *et al.*, 2001; Soetens *et al.*, 2001; Springael *et al.*, 1999). Ubiquitination constitutes a common signal for endocytic internalization of a variety of plasma membrane proteins (reviewed by Hicke, 1997; Horák, 2003). The second category includes mutations that cause constitutive sorting of Gap1p to the vacuole, regardless of the nitrogen source in the growth medium. Among the genes belonging to this category are the genes *LST4*, *LST7*, and *LST8*, which were initially identified because of their lethality in combination with a thermosensitive allele of *SEC13* (Roberg *et al.*, 1997b). *LST8* encodes a positively acting component of the TOR pathway that affects Gap1p sorting by negatively regulating the transcription factors Rtg1/3p and Gln3p, thereby limiting the synthesis of α-ketoglutarate, glutamate, and glutamine (Chen and Kaiser, 2003). The roles of *LST4* and *LST7* have not been elucidated. A fundamental relationship between mutations of the two types is that, when a mutation that blocks ubiquitination and causes constitutive sorting to the plasma membrane is combined with a mutation that causes constitutive sorting to the vacuole, the double mutants invariably show constitutive sorting to the plasma membrane. This finding has led to the hypothesis that ubiquitination of Gap1p precedes sorting of Gap1p to a compartment in which the mutations of the second type can exert their effect (Helliwell *et al.*, 2001).

A variety of studies have revealed that sorting of most plasma membrane proteins for degradation in the vacuolar lumen occurs through the maturation of the late endosome or prevacuolar compartment into multivesicular endosomes (MVEs; reviewed by Katzmann *et al.*, 2002; Raiborg *et al.*,

This article was published online ahead of print in *MBC in Press* (http://www.molbiolcell.org/cgi/doi/10.1091/mbc.E05–07–0669) on April 26, 2006.

Address correspondence to: Chris A. Kaiser (ckaiser@mit.edu).

2003; Babst, 2005). The protein machinery required for MVE formation was discovered by identification of class E *vps* mutants. These mutants share a common phenotype characterized by accumulation of proteins destined for the vacuole in an enlarged prevacuolar (class E) compartment (Raymond *et al.*, 1992). Most of the class E *VPS* (vacuolar protein sorting) genes encode components of three protein complexes (endosomal sorting complex required for transport [ESCRT]), designated ESCRTI, ESCRTII, and ESCRTIII, which are required for the formation of inwardly budding luminal vesicles that fill the interior of MVEs. The luminal vesicles typically contain membrane proteins that arrive in the prevacuolar compartment either by vesicular trafficking from the Golgi or by endocytosis and are eventually degraded completely in the vacuole lumen. Mutations in ESCRT complex prevent formation of inwardly budding vesicles, leading to formation of a class E compartment rather than a MVE. Impaired formation of inwardly budding vesicles can block recycling of proteins such as Vps10p from the prevacuolar compartment to the Golgi, thus leading to their accumulation in the resulting class E compartment (Babst *et al.*, 1998, 2000, 2002a, 2002b; Babst, 2005; Katzmann *et al.*, 2001, 2003; Bilodeau *et al.*, 2003; Odorizzi *et al.*, 2003; Luhtala and Odorizzi, 2004).

Most membrane proteins that are normally delivered to the lumen of the vacuole require modification by ubiquitination as a signal for being packaged into luminal vesicles of the MVE. Recent work has demonstrated that in many cases Rsp5p is directly required at the MVEs for modification and adequate sorting of membrane proteins (Blondel *et al.*, 2004; Dunn *et al.*, 2004; Katzmann *et al.*, 2004; Morvan *et al.*, 2004). Instead of causing an increase in plasma membrane sorting, as observed for Gap1p (Helliwell *et al.*, 2001), in these cases an *rsp5* mutation causes the cargo to accumulate in the delimiting membranes of the endosomal and vacuolar compartments.

Deubiquitination of the MVE cargo before its internalization into luminal vesicles is also important for the proper sorting of MVE cargo proteins. For example, The ubiquitin (Ub) C-terminal hydrolase encoded by *DOA4* plays a major role at this step in the deubiquitination of different MVE cargoes. A *doa4*Δ mutation causes mistargeting of MVE cargo proteins and a failure to recycle ubiquitin, which results in depletion of intracellular pools of free ubiquitin (Swaminathan *et al.*, 1999; Amerik *et al.*, 2000; Dupré and Haguenauer-Tsapis, 2001).

Although defects in cargo ubiquitination, recognition by ESCRT machinery, and deubiquitination at the MVEs may result in the accumulation of proteins in endosomal and perivacuolar membranes, recent studies indicate the existence of alternative pathways that allow recycling of plasma membrane proteins from the latest stages of lysosomal/vacuolar sorting (Babst *et al.*, 2000; Nikko *et al.*, 2003; Bugnicourt *et al.*, 2004; Pizzirusso and Chang, 2004).

Here we present the results of a genome-wide screen used to identify new functions involved in the control of Gap1p intracellular sorting. We find that mutations in all of the class E *VPS* genes involved in the MVE pathway cause missorting of intracellular Gap1p to the plasma membrane. Our results show both that Gap1p must follow the MVE pathway in order to be delivered to the vacuole and that a deficiency in the MVE machinery allows efficient retrieval of Gap1p from this intracellular compartment (probably via the *trans*-Golgi) to the plasma membrane rather than causing its accumulation in the class E compartment. Evaluation of the Gap1p sorting in cells grown on different nitrogen sources shows that cycling of Gap1p from the MVE to the plasma membrane is the main step in the intracellular trafficking itinerary of Gap1p that is regulated by amino acids.

MATERIALS AND METHODS

Strains, Plasmids, and Media

A genome-wide screen was performed using the collection of *kanMX*-marked deletion mutants in nonessential genes of *S. cerevisiae*, from EUROSCARF (http://www.uni-frankfurt.de/fb15/mikro/euroscarf/data/by.html; Brachmann *et al.*, 1998). All the null mutants utilized in our screen are in the BY4741 (Y00000) and BY4742 (Y10000) genetic backgrounds (*MAT***a** *his3*Δ*1 leu2*Δ*2 met15*Δ*0 ura3*Δ*0* and *MAT*α *his3*Δ*1 leu2*Δ*2 lys2*Δ*0 ura3*Δ*0*, respectively). Characteristically, strains of this genetic background (derived from S288C) produce high Gap1p and Put4p activity when ammonia is used as nitrogen source (Courchesne and Magasanik, 1983). All of the mutants assayed for Gap1p activity and localization were reconstructed in our laboratory genetic background, also derived from S288C, and are listed in Table 1. All complete gene deletions described here were obtained by replacement of the functional ORF of the corresponding gene by homologous recombination with either a *kanMX4/6* or a *natMX4* cassette (Longtine *et al.*, 1998; Goldstein and McCusker, 1999) in the wild-type strain CKY835.

Plasmids used in this study are summarized in Table 2. Plasmids previously available in the Kaiser collection used for this work are as follows: pRS423, *HIS3* 2 μ (Christianson *et al.*, 1992); pRS415, a *LEU2-CEN* vector (Sikorski and Hieter, 1989); pP_{GAP1}*-lacZ* (pMS29), a centromeric plasmid carrying a P_{GAP1}*-LacZ* fusion at codon 53 of *GAP1* in the *URA3-CEN* vector pBL101 (Stanbrough and Magasanik, 1995); p*GAP1-GFP* (pCK230), a *URA-CEN* vector carrying the GAP1-sGFP fusion under the *GAP1* promoter (Helliwell *et al.*, 2001); and p*BUL1* (pCK323), an *HIS3* 2 μ pRS423 plasmid containing *BUL1* ORF plus 5′ and 3′ regions. To make the centromeric plasmid covering for leucine, histidine, and methionine auxotrophies, p*CEN-HIS3-LEU2-MET15* (pCK283), a DNA fragment containing the *HIS3* marker from pRS423 (Christianson *et al.*, 1992), flanked by the restriction sites SacI and SalI, was obtained by PCR and introduced in the plasmid pRS415 (Sikorski and Hieter, 1989). A PCR fragment containing *MET15* was obtained by genomic PCR from CKY835. Both the fragment and the intermediate vector (containing *LEU2* and *HIS3* markers), previously digested with ApaI, were treated with T4-DNA polymerase before the ligation. To construct the plasmids pP_{CUP1}*-myc-UBI* (pCK322) and pP_{CUP1}*-UBI* (pCK331), a BamHI-ClaI fragment containing the copper-inducible ubiquitin cassette P_{CUP1}*-myc-UBI* amplified from pCK231 plasmid (Helliwell *et al.*, 2001) or P_{CUP1}*-UBI* amplified from YEP96 plasmid (Ecker *et al.*, 1987; Ellison and Hochstrasser, 1991) were, respectively, ligated to BamHI/ClaI-digested pRS306 2 μ, for *URA3* selection (Sikorski and Hieter, 1989; Helliwell *et al.*, 2001). *Escherichia coli* DH5α was used for each cloning step. The rest of the genetic and DNA manipulation general procedures were performed according to the protocols described in Sambrook *et al.* (1997) and Adams *et al.* (1996).

The defined growth media are based on Yeast Nitrogen Base (Difco, Detroit, MI) and designated according to the nitrogen source added (urea, ammonia, or glutamate), and the composition and preparation are as described by Roberg *et al.* (1997a). All growth experiments were carried out at 24°C. Plates containing the toxic proline analog L-azetidine-2-carboxylic acid (ADCB; Sigma-Aldrich, St. Louis, MO) were prepared by using minimal medium with ammonia or urea as the only nitrogen source. When auxotrophic EUROSCARF strains were used, minimal medium was supplemented appropriately with amino acids, purines, or pyrimidines, added at concentrations given in Adams *et al.* (1996).

Assays for Amino Acid Uptake and β-Galactosidase

Assays of the rate of uptake of radiolabeled amino acids were performed as described by Roberg *et al.* (1997b). β-Galactosidase activity was measured using the permeabilized cell method (Adams *et al.*, 1996).

Screen for Mutations That Affect Gap1p Activity

A primary screen was performed using master 96-well microtiter dishes containing the entire collection of deletions in nonessential genes of the EUROSCARF collection. Approximately 4859 BY strains of each haploid mating type were grown on solid YPD medium overnight and transferred to 96-well plates. Strains were spotted onto plates of minimal urea medium supplemented with amino acids and containing five different concentrations (0, 8, 30, 60, 100 mg/l) of ADCB. Sensitivity or resistance to ADCB was scored after growth for 3–4 d. As controls on each screening plate, we used the wild-type standard strain, BY4741 (Y00000) and the mutant strains *lst4*Δ (Y05026), which causes reduced levels of Gap1p activity (Roberg *et al.*, 1997b), and *gln3*Δ (Y00173), which causes increased levels of Gap1p activity (Stanbrough and Magasanik, 1995; Chen and Kaiser, 2002). Candidate strains with either increased sensitivity or resistance to ADCB were reconfirmed in both mating types (BY4741 and BY4742 backgrounds). Subsequent to the initial screening of the deletion strains, Gap1p activity and transcription were determined after transformation of strains with pCK283 to render the

Table 1. *S. cerevisiae* strains isogenic with S288C used in this study (listed as appeared in the text)

Strain	Genotype	Source[a]
CKY835	MATα *ura3–52*	This study
CKY695	MATα *lst4Δ::kanMX6 ura3-52*	KSC
CKY698	MAT**a** *bul1Δ::kanMX6 bul2Δ::kanMX6 ura3-52*	KSC
CKY839	MAT**a** *did4Δ::kanMX4 ura3-52*	This study
CKY836	MATα *vps4Δ::kanMX4 ura3-52*	This study
CKY837	MATα *vps27Δ::kanMX4 ura3-52*	This study
CKY838	MATα *doa4Δ::kanMX4 ura3-52*	This study
CKY833	MAT**a** P_{ADH1}*-GAP1::kanMX6*	KSC
CKY840	MATα P_{ADH1}*-GAP1::kanMX6 did4Δ::kanMX4*	This study
CKY841	MATα P_{ADH1}*-GAP1::kanMX6 vps4Δ::kanMX4*	This study
CKY842	MATα P_{ADH1}*-GAP1::kanMX6 vps27Δ::kanMX4 ura3-52*	This study
CKY843	MAT**a** P_{ADH1}*-GAP1::kanMX6 doa4Δ::kanMX4 ura3-52*	This study
CKY834	MAT**a** *GAP1-GFP::kanMX6*	KSC
CKY758	MAT**a** *mks1Δ::kanMX6*	KSC
CKY923	MATα *mks1Δ::kanMX6 bul1Δ::kanMX6 bul2Δ::kanMX6*	KSC
CKY924	MATα *mks1Δ::kanMX6 vps27Δ::kanMX4*	This study
CKY867	MAT**a** *GAP1-GFP::kanMX6 mks1Δ::kanMX6*	KSC
CKY926	MATα *GAP1-GFP::kanMX6 mks1Δ::kanMX6 bul1Δ::kanMX6 bul2Δ::kanMX6 ura3-52*	This study
CKY927	MATα *GAP1-GFP::kanMX6 mks1Δ::kanMX6 vps27Δ::kanMX4*	This study
CKY925	MATα *GAP1-GFP::kanMX6 bul1Δ::kanMX6 bul2Δ::kanMX6*	This study
CKY851	MAT**a** *GAP1-GFP::kanMX6 vps27Δ::kanMX4 ura3-52*	This study
CKY934	MATα *end3Δ::kanMX6*	KSC
CKY847	MAT**a** *lst4Δ::natMX4 doa4Δ::kanMX4 ura3-52*	This study
CKY935	MATα *bro1Δ::natMX4*	This study
CKY936	MATα *lst4Δ::kanMX6 bro1Δ::natMX4 ura3-52*	This study
CKY844	MATα *lst4Δ::natMX4 did4Δ::kanMX4 ura3-52*	This study
CKY845	MATα *lst4Δ::natMX4 vps4Δ::kanMX4 ura3-52*	This study
CKY846	MAT**a** *lst4Δ::natMX4 vps27Δ::kanMX4 ura3-52*	This study
CKY699	MATα *lst4Δ::kanMX6 bul1Δ::kanMX6 bul2Δ::kanMX6 ura3-52*	KSC
CKY848	MAT**a** *GAP1-GFP::kanMX6 lst4Δ::kanMX6 ura3-52*	This study
CKY850	MAT**a** *GAP1-GFP::kanMX6 vps4Δ::kanMX4*	This study
CKY849	MAT**a** *GAP1-GFP::kanMX6 did4Δ::kanMX4*	This study
CKY937	MATα *GAP1-GFP::kanMX6 bro1Δ::natMX4 ura3-52*	This study
CKY854	MATα *GAP1-GFP::kanMX6 lst4Δ::kanMX6 vps4Δ::kanMX4*	This study
CKY855	MATα *GAP1-GFP::kanMX6 lst4Δ::kanMX6 vps27Δ::kanMX4 ura3-52 leu2-3,112*	This study
CKY853	MATα *GAP1-GFP::kanMX6 lst4Δ::natMX4 did4Δ::kanMX4*	This study
CKY938	MATα *GAP1-GFP::kanMX6 lst4Δ::kanMX6 bro1Δ::natMX4 ura3-52*	This study
CKY857	MATα *did2Δ::kanMX4 ura3-52*	This study
CKY858	MATα *hse1Δ::kanMX4 ura3-52*	This study
CKY859	MATα *vps23Δ::kanMX4 ura3-52*	This study
CKY860	MATα *vps37Δ::kanMX4 ura3-52*	This study
CKY861	MATα *vps60Δ::kanMX4 ura3-52*	This study
CKY995	MATα *vps5Δ::kanMX4 vps4Δ::natMX4 ura3*	This study
CKY996	MATα *vps26Δ::kanMX4 vps4Δ::natMX4 ura3*	This study
CKY997	MAT**a** *vps51Δ::kanMX4 vps4Δ::natMX4 ura3*	This study
CKY998	MATα *vps52Δ::kanMX4 vps4Δ::natMX4 his3Δ1 leu2Δ2 met15Δ0 ura3*	This study
CKY999	MATα *vps16Δ::kanMX4 vps4Δ::natMX4 ura3*	This study
CKY1000	MATα *vps18Δ::kanMX4 vps4Δ::natMX4 met15Δ0 ura3*	This study
CKY1001	MAT**a** *ypt6Δ::kanMX4 vps4Δ::natMX4 ura3*	This study
CKY1002	MAT**a** *ypt7Δ::kanMX4 vps4Δ::natMX4 met15Δ0 ura3*	This study
CKY1003	MATα *vam3Δ::kanMX4 vps4Δ::natMX4 ura3*	This study
CKY1004	MATα *vps33Δ::kanMX4 vps4Δ::natMX4 ura3*	This study
CKY994	MAT**a** *lst7Δ::kanMX4 ura3-52*	KSC
CKY1005	MAT**a** *lst7Δ::kanMX4 vps4Δ::kanMX4 ura3–52*	This study
CKY874	MATα *end3Δ::kanMX6 GAP1-GFP::kanMX6*	This study
CKY875	MAT**a** *end3Δ::kanMX6 lst4Δ::kanMX6 GAP1-GFP::kanMX6 ura3-52*	This study
CKY694	MATα *pep12Δ::TRP1 ura3*	KSC
CKY1006	MAT**a** *lst4Δ::kanMX6 pep12Δ::TRP1 ura3*	KSC
CKY1007	MATα *gga1Δ::kanMX4 gga2Δ::kanMX4 ura3*	This study
CKY1008	MAT**a** *lst4Δ::natMX4 gga1Δ::kanMX4 gga2Δ::kanMX4 ura3*	This study
CKY852	MAT**a** *doa4Δ::kanMX4 GAP1-GFP::kanMX6 ura3-52*	This study
CKY868	MATα P_{ADH1}*-GAP1-HA::kanMX6 pep4Δ::LEU2 ura3-52 leu2-3,112*	This study
CKY928	MATα *doa4Δ::kanMX4* P_{ADH1}*-GAP1-HA::kanMX6 pep4Δ::LEU2 ura3-52*	This study
CKY930	MATα *doa4Δ::natMX4 bul1Δ::kanMX6 bul2Δ::kanMX6* P_{ADH1}*-GAP1-HA::kanMX6 pep4Δ::LEU2 ura3–52 leu2-3,112*	This study
CKY474	MATα *pep4Δ::LEU2 ura3-52 leu2-3,112*	KSC
CKY993	MAT**a** *doa4Δ::natMX4 pep4Δ::LEU2 ura3–52 leu2-3,112*	This study
CKY929	MATα *doa4Δ::natMX4* P_{ADH1}*-gap1*$^{K9R,\ K16R}$*-HA::kanMX6 pep4Δ::LEU2 ura3-52*	This study
CKY931	MATα *doa4Δ::kanMX4 lst4Δ::natMX4* P_{ADH1}*-GAP1-HA::kanMX6 pep4Δ::LEU2 ura3-52 leu2-3,112*	This study
CKY1009	MAT**a** *doa4Δ::natMX4* P_{ADH1}*-GAP1-HA::kanMX6 pep4Δ::LEU2 his3Δ0 ura3-52 leu2-3,112*	This study

[a] KSC, Kaiser Strain Collection.

Table 2. Plasmids used in this study

Genotype	Name	Other name, description
	pRS415	*LEU2 CEN* (Sikorski and Hieter, 1989)
	pRS423	*HIS3* 2μ (Christianson *et al*., 1992)
p*CEN-HIS3-LEU2-MET15*	pCK283	pMRT2; *HIS3* and *MET15* genes inserted in pRS415
pP_{GAP1}-*lacZ*	pMS29	P_{GAP1}-*lacZ* fusion at codon 53 of *GAP1*; *CEN* (Stanbrough and Magasanik, 1995)
p*GAP1-GFP*	pCK230	pSH40; *GAP1-sGFP* fusion under the *GAP1* promoter; *CEN* (Helliwell *et al*., 2001)
pP_{CUP1}-*myc-UBI*	pCK322	pMRT7; pRS306 2μ containing P_{CUP1}-*myc-UBI* expression cassette
pP_{CUP1}-*UBI*	pCK331	pMRT15; pRS306 2μ containing P_{CUP1}-*UBI* expression cassette
p*BUL1*	pCK323	pSH53; pRS423 containing BUL1 ORF plus 5′ and 3′ regions

strains prototrophic (so that amino acid supplements would not be necessary in the growth medium) and with pMS29 as a reporter to monitor *GAP1* expression.

Fluorescence Microscopy

Labeling with FM4-64 (Molecular Probes, Eugene, OR) was performed according to the procedure described in Vida and Emr (1995). For GFP localization studies, Gap1p-GFP–expressing cells were grown to exponential phase in ammonia liquid cultures. Glutamate was added to a final concentration of 3 mM and the cells were incubated for 30 min to 1 h at 24°C. Cells were then collected by centrifugation, washed, and suspended in 1 M Tris, pH 8.0, 5% NaN_3 as described by Urbanowski and Piper (1999). This treatment stops the membrane traffic and provides alkaline conditions optimal for GFP fluorescence imaging. Images were captured with a Nikon E800 microscope (Melville, NY) equipped with a Hamamatsu digital camera (Bridgewater, NJ). The FITC filter set was used for imaging of FM4-64 detection and the chroma filter set at 41012 was used for GFP detection. Improvision OpenLabs 2.0 software (Lexington, MA) was used to process images.

FM4-64 Recycling Assay

To measure recycling of endocytosed membranes back to the cell surface, we carried out FM4–64 recycling assays as described in Wiederkehr *et al.* (2000). Fluorescence was recorded using a Fluorolog spectrofluorometer (Jobin/Yvon, Horiba, Irvine, CA).

Carboxy peptidase Y Secretion Assay

Detection of secreted carboxy peptidase Y (CPY) was carried out as described by Lafourcade *et al.* (2004).

Immunoprecipitation and Immunoblotting of Ubiquitin Conjugates of Gap1p

For the detection of Gap1 protein levels, two OD_{600} of cells were collected at the required times after shifting nitrogen sources and protein extracts carried out by following a protocol from Adams *et al.* (1996). Proteins were resolved by 8% SDS-PAGE and detected by immunoblot using rabbit polyclonal anti-Gap1p antibody (made as explained in Risinger and Kaiser, unpublished results) at 1:2000 dilution, mouse monoclonal anti-3-phosphoglycerate kinase (1:1000, Molecular Probes) used for simultaneous detection of Pgk1p as a loading control, and HRP-conjugated donkey anti-rabbit IgG or HRP-coupled sheep anti-mouse IgG (1:10,000 dilution, Amersham, Indianapolis, IN).

For the detection of Gap1p-HA and its ubiquitin conjugates, Gap1p was immunoprecipitated and then detected by immunoblotting following an adaptation of the protocol described by Laney and Hochstrasser (2002). Strains were transformed with pP_{CUP1}-*myc-UBI* (pCK322) and then cultured in minimal urea medium to an initial OD_{600} of 0.01/ml. *myc*-Ubi expression was induced for 16 h with 1 μM $CuSO_4$. An equivalent to 10 OD_{600} units of cells were collected on 0.45-μm nitrocellulose filters once cultures reached 0.4 OD_{600}/ml. Cells were washed twice in 10 mM NaN_3, suspended in 200 μl of SDS buffer containing NEM and protease inhibitors (1% (wt/vol) SDS; 45 mM Na-HEPES, pH 7.5; 50 mM NEM; 1 mM phenylmethylsulfonyl fluoride (PMSF); 0.5 μg/ml leupeptin, 2 μg/ml aprotinin, and 0.7 μg/ml pepstatin), and lysed with glass beads by vortexing 5 min at room temperature. Lysates were diluted in 700 μl of Triton lysis buffer with NEM and protease inhibitors (1% [vol/vol] Triton X-100; 150 mM NaCl; 50 mM Na-HEPES, pH 7.5; 5 mM Na-EDTA; 10 mM NEM; 1 mM PMSF; 0.5 μg/ml leupeptin; 2 μg/ml aprotinin, and 0.7 μg/ml pepstatin), and any remaining cell debris was removed by centrifugation at 4°C, 14,000 $\times$ *g*. Samples were preadsorbed for 1 h at room temperature with 40 μl of a 20% suspension of protein G-Sepharose 4 fast flow (Amersham Pharmacia Biotech, Piscataway, NJ) followed by brief centrifugation to remove the beads. This procedure was repeated twice. Immunoprecipitation was carried out by overnight incubation at 4°C with 10 μl of monoclonal antibody preparation (rat anti-HA [3F10]; Roche, Indianapolis, IN), followed by overnight incubation at 4°C with 60 μl of protein G-Sepharose suspension. The beads were washed five times with 1% (vol/vol) Triton in phosphate-buffered saline buffer containing NEM 10 mM, 1 mM PMSF, 0.5 μg/ml leupeptin, 2 μg/ml aprotinin, and 0.7 μg/ml pepstatin. Immunoprecipitates were solubilized by incubation in sample buffer for 1 h at 37°C and resolved by 8% SDS-PAGE. Antibodies used for immunoblotting included mouse anti-HA monoclonal 16B12 (BAbCO, Richmond, CA) at 1: 1000 dilution; mouse anti-*myc*, monoclonal 9E10 (Santa Cruz Biotechnology, Santa Cruz, CA) at 1: 500 dilution; and HRP-coupled sheep anti-mouse serum at 1: 10,000 dilution (Amersham Pharmacia).

Pulse-Chase Experiments

To assess the inhibition of bulk translation caused by cycloheximide, cells growing exponentially in minimal glutamate medium lacking methionine were suspended in fresh medium at 5 OD_{600}/ml and pulse-labeled for 4 min by addition of 30 μCi of [^{35}S]methionine and [^{35}S]cysteine (EXPRESS, NEN, Boston, MA) per OD_{600}. Cycloheximide was then added and cells were incubated for 30 min at room temperature. Metabolic labeling of proteins was stopped by the addition of unlabeled 10 mM methionine and 10 mM cysteine before washing twice with ice-cold 20 mM NaN_3. A 0.4-ml aliquot of culture was suspended in 200 μl of sample buffer containing protease inhibitors as above. Cells were lysed by vortexing with glass beads for 5 min at 4°C, and boiled for 1 min, 20-μl samples were resolved by SDS-PAGE (8% gel), and labeled proteins were detected with a 445si PhosphorImager (Molecular Dynamics, Sunnyvale, CA).

RESULTS

Identification of VPS Genes Involved in the Sorting of Gap1p

To identify new genes that govern proper sorting of nitrogen-regulated permeases, we screened 4859 haploid deletion mutants in nonessential genes of *S. cerevisiae* from the EUROSCARF collection. For the first step of selection in this screen we used the toxic proline analog ADCB, which is taken up primarily by Gap1p and Put4p permeases in cells grown on ammonia or urea as a nitrogen source (Roberg *et al.*, 1997a). Mutations causing increased Gap1p and Put4p activities display enhanced sensitivity to ADCB, whereas mutations that reduce these activities are more resistant to this compound (Roberg *et al.*, 1997b). By spotting each strain from the collection onto plates with minimal urea medium containing different concentrations of ADCB, a total of 162 mutants showing sensitivity to a normally sub-LC (<12.5 mg/l) of ADCB were identified. (An additional 118 mutants that displayed resistance to ADCB were identified, and these mutants will be described elsewhere.)

Enhanced sensitivity to ADCB, indicating increased activity of Gap1p and Put4p could be due to an effect on either the intracellular sorting of nitrogen-regulated permeases or their level of expression. To distinguish these possibilities, we assayed the effect of each mutant on Gap1p activity and expression. Gap1p activity was measured by the rate of uptake of [^{14}C]citrulline, which is transported only by Gap1p. For these experiments, uptake of [^{14}C]arginine was used to control for nonspecific effects on permease activity. *GAP1* transcription was evaluated by measuring the β-galactosidase activity expressed from a P_{GAP1}-*lacZ* reporter.

Table 3. Mutants in genes involved in vacuolar protein sorting assayed for ADCB sensitivity

Gene/parental strain name[a]	Proposed function in the literature/databases	Growth of deletion mutant on ADCB[b]
BY4741	Wild type	+
CLASS A		
PEP1/VPS10	Sorting receptor for soluble vacuolar proteins	+/−
VPS13	Late endosome to vacuole transport	+
VPS29	Retromer complex (retrograde transport endosome to Golgi)	+
VPS30	Sorting of soluble hydrolases to vacuole; required for autophagy	+
VPS35	Retromer complex (retrograde transport endosome to Golgi)	+
VPS38	Mediates interaction between Vps30 and Vps34p-Vps15p; late endosome to vacuole transport	+
VPS63	Dubious ORF, 98% overlaps the gene *YPT6*; involved in CPY sorting/trafficking	+
VPS74	CPY and Pep4p trafficking to the vacuole; apical bud growth	+
CLASS B		
VAM3	Syntaxin homolog (t-SNARE), required for vacuolar assembly	+
VPS5	Retromer complex (retrograde transport endosome to Golgi)	+
VPS17	Retromer complex (retrograde transport endosome to Golgi)	+
VAM6/VPS39	HOPS complex	+
VPS41	HOPS complex	+
VAM7/VPS43	Vacuolar SNARE complex	+
VPS52	Subunit of the VFT/GARP complex, involved in retrograde transport, endosome to Golgi	+
VPS53	Subunit of the VFT/GARP complex, involved in retrograde transport, endosome to Golgi	+
VPS54	Subunit of the VFT/GARP complex, involved in retrograde transport, endosome to Golgi	+
VPS51/VPS67	Subunit of the VFT/GARP complex, involved in retrograde transport, endosome to Golgi	+
VPS61	Deletion causes defects in CPY and Pho8p trafficking to the vacuole	+
VPS64/FAR9	CPY trafficking and α-factor secretion	+
VPS66	CPY vacuolar trafficking pathway	−
VPS69	CPY vacuolar trafficking pathway	+/−
VPS71	Component of the Swr1p complex; CPY vacuolar trafficking pathway	−
VPS72	Component of the Swr1p complex; CPY vacuolar trafficking pathway	−
VPS73	Mitochondrial protein of unknown function involved in vacuolar protein sorting	+
VPS75	CPY and Pho8p trafficking to the vacuole	+
CLASS C		
PEP5/VPS11	HOPS complex	+
VPS16	HOPS complex	+/−
PEP3/VPS18	HOPS complex	−
VPS33	HOPS complex	+
CLASS D		
VPS3	Vacuolar sorting and segregation	−
VPS8	Retrieval of Golgi membrane proteins from prevacuolar compartment	+
PEP12/VPS6	Syntaxin homolog (t-SNARE) involved in Golgi to vacuole transport	−
VPS9	Required for Golgi to vacuole transport	+
VPS15	Myristoylated Ser/Thr protein kinase possibly involved in the activation of Vps34p	+
PEP7/VPS19	Vacuolar segregation and acidification	−
VPS21	Rab5-like GTPase required for sorting of vacuolar proteins	+
VPS34	Phosphatidyl inositol (PI) 3-kinase required for vacuolar protein sorting	+
VPS45	Protein of the Sec1p family, essential for vacuolar protein sorting	+
Class E		
DID2/FTI1	Small coiled-coil protein; human ortholog may be altered in breast tumors	+/−
VPS60/MOS10	Small coiled-coil protein with notable identity to *VPS32* and *VPS20*	+/−
HSE1	Sorting of ubiquitinated cargo into MVEs; interacts with Vps27p	+
VPS27	Sorting of ubiquitinated cargo into MVEs; recruits/activates ESCRT-I on endosomes	−
STP22/VPS23	ESCRT-I complex component (MVE sorting pathway)	−
VPS28	ESCRT-I complex component (MVE sorting pathway)	−
SRN2/VPS37	ESCRT-I complex component (MVE sorting pathway)	−
SNF8/VPS22	ESCRT-II complex component (MVE sorting pathway)	−
VPS25	ESCRT-II complex component (MVE sorting pathway)	−
VPS36	ESCRT-II complex component (MVE sorting pathway)	−
SNF7/VPS32	ESCRT-III complex component (subcomplex with Vps20p; MVE sorting pathway)	−
VPS20	ESCRT-III complex component (subcomplex with Vps32p; MVE sorting pathway)	−
DID4/VPS2	ESCRT-III complex component (MVE sorting pathway)	−
VPS24	ESCRT-III complex component (subcomplex with Vps2p)	−
VPS4	AAA ATPase protein; release of ESCRT complexes from endosomal membranes	−
BRO1/VPS31	Necessary for efficient recruitment of Doa4p into endosomes	−
NHX1/VPS44	Na+/H+ antiporter required for endosomal trafficking	−
Class F		
VPS1	GTPase; vacuolar sorting and retention of Golgi proteins	+
PEP8/VPS26	Retromer complex (retrograde transport endosome to Golgi)	+
VPS55	Late endosome to vacuole trafficking	+

Continued

Table 3. *Continued*

Gene/parental strain name[a]	Proposed function in the literature/databases	Growth of deletion mutant on ADCB[b]
VPS62	CPY and Pep4p trafficking to the vacuole	+
VPS65	Dubious ORF; vacuolar protein sorting; actin organization	−
VPS68	CPY and Pep4p trafficking to the vacuole	+
VPS70	Vacuolar protein sorting; protease associated domain	+
Others		
FAB1	PI(3)P-5 kinase involved in MVE formation	+
DEF1/VID31	Protein involved in vacuolar import and degradation	+/−
DOA4	Ub C-terminal hydrolase; recycling of Ub from protein substrates	−
TUL1	Transmembrane Ub-ligase involved in the ubiquitination of misfolded membrane proteins	+
PIB1	E2-dependent Ub ligase resident of endosomal and vacuolar membranes	+

[a] Genes are listed according to the *Saccharomyces* Genome Database (the most common alias has also been included for some of them).

[b] Growth is represented according to the survival of the mutant strains on plates of minimal urea medium with different concentrations of ADCB: +, mutants with wild type behavior, unable to grow in concentrations above 30 mg/l; +/−, moderately sensitive mutants unable to grow in concentrations above 12.5 mg/l; −, hypersensitive mutants unable to grow above 7 mg/l. Sublethal concentrations for the control strains were 6.25 mg/l for a *gln3*Δ mutant and >100 mg/l for an *lst4*Δ mutant.

These assays showed that 73 of the mutants had significantly increased Gap1p activity, and that for 70 of these mutants the increase in Gap1p activity was not due to an increase in *GAP1* transcription (our unpublished data). Among the mutants that displayed increased Gap1p activity but normal *GAP1* transcription, we almost the entire set of class E of *VPS*, which code for members of the ESCRT machinery acting at the MVE (Babst, 2005). The phenotypes obtained in the ADCB screen for mutations in all known *VPS* genes are summarized in the Table 3.

As shown in Table 4, most class E *vps* mutants showed 10- to 30-fold increases in Gap1p activity on urea medium, suggesting a greatly increased probability of sorting of the permease to the cell surface. Moreover, the deletion of *DOA4*, which causes a depletion of the pools of free ubiquitin, also caused increased levels of Gap1p activity. None of the mutations in this subset of genes caused a corresponding increase in the uptake of arginine, suggesting that their effect was specific for Gap1p. Similar results were observed when the same *VPS* genes were deleted in an S288C strain prototrophic for amino acids (CKY strains; Table 1). These mutants showed an inability to grow on plates of minimal urea medium containing 7 mg/l of ADCB, as shown for *did4*Δ, *vps4*Δ, *vps27*Δ, and *doa4*Δ (Figure 1A). Uptake assays revealed from 10- to 20-fold increases in Gap1p activity compared with the wild-type strain in the same medium (Figure 1B). This increase in Gap1p activity was about the same as that for a *bul1*Δ *bul2*Δ double mutant, which causes a 30-fold increase in Gap1p activity on urea medium (Figure 1B).

To examine the mutational effects on Gap1p trafficking, exclusive of any influence on *GAP1* gene transcription, we placed the *GAP1* coding sequence under control of the constitutive *ADH1* gene promoter, which is unaffected by the amino acids regulatory signal (Chen and Kaiser, 2002; Figure 1C). All of the class E *vps* mutants exhibited 10- to 20-fold increased levels of activity expressed from P_{ADH1}-*GAP1*, showing that the increase in Gap1p activity was not due to changes in transcriptional regulation. Together, these results show that mutations in components of the MVE machinery can cause a dramatic redistribution of Gap1p to the plasma membrane.

Membrane proteins targeted to the vacuole through the MVE pathway are sorted into the membrane of inwardly budding vesicles generated at the MVE, which are ultimately delivered into the vacuolar lumen when the MVE fuses with the vacuole (Reggiori and Pelham, 2001; Katzmann *et al.*, 2002; Babst, 2005). Accordingly, Gap1p-GFP in a wild-type strain growing in a high concentration of the amino acid glutamate, which induces Gap1p vacuolar sorting, localizes within the vacuolar lumen (Figure 2).

These results suggest that functional MVE machinery is necessary for the vacuolar sorting of the nitrogen-regulated amino acid permeases and that defects in the MVE pathway can lead to efficient delivery of Gap1p to the cell surface.

Gap1p Sorting Responds to Amino Acids in MVE Mutants

We asked whether the increased levels of Gap1p activity in class E *vps* mutants might be due to a defect in responding to amino acids. Mutations in *MKS1* display high, unregulated expression of TCA pathway enzymes responsible for α-ketoglutarate formation and thus produce high levels of glutamate and glutamine (Butow and Avadhani, 2004). We have found that high amino acid content of *mks1*Δ mutants cause Gap1p to be sorted to the vacuole (Chen and Kaiser, 2002). Mutants defective in Gap1p polyubiquitination, when combined with *mks1*Δ, showed highly increased levels of active Gap1p localized to the cell surface (as observed in Figure 3, A and B, for the triple mutant *mks1*Δ *bul1*Δ *bul2*Δ). This result establishes that if Gap1p cannot be ubiquitinated, that Gap1p sorting no longer responds to high levels of amino acids. By contrast, a double mutant *mks1*Δ *vps27*Δ exhibited low levels of Gap1p activity (Figure 3A). Examination of Gap1p-GFP in *mks1*Δ *vps27*Δ strains revealed that Gap1p-GFP accumulated in endosomal/perivacuolar membranes, suggesting that Gap1p rerouting to the vacuolar sorting pathway in response to high internal amino acid concentrations is not impaired in this double mutant (Figure 3B).

Because the class E *vps* mutants exhibited high Gap1p activity and localization of Gap1p-GFP to the plasma membrane, we also considered the possibility that class E *vps* mutants might be defective for Gap1p endocytosis from the plasma membrane. We tested three representative class E mutants (*vps4*Δ, *vps27*Δ, and *did4*Δ) for a rate of decline in Gap1p activity, indicative of functional endocytosis, right after the addition of 3 mM glutamate to cells growing in ammonia medium (Figure 3C). Although cells continuously growing in the absence of amino acids maintained relatively high levels of Gap1p activity, addition of glutamate caused a decline in

Table 4. Effect on Gap1p activity of vacuolar sorting mutants selected in the genomic screen

Gene	Proposed function for the encoded protein	Growth on ADCB[a]	Gap1p activity (%)[b]	Arginine uptake (%)
BY4741	Wild type	+	100 ± 13	100 ± 04
CLASS A				
VPS29	Retromer complex	+	436 ± 103	82 ± 11
VPS35	Retromer complex	+	309 ± 51	107 ± 01
CLASS B				
VAM3	Homotypic vacuolar fusion	+	327 ± 51	111 ± 13
VPS5	Retromer complex	+	418 ± 121	121 ± 23
VPS17	Retromer complex	+	73 ± 13	97 ± 04
VPS52	VFT/GARP complex	+	336 ± 39	70 ± 03
VPS53	VFT/GARP complex	+	345 ± 26	68 ± 05
VPS54	VFT/GARP complex	+	340 ± 16	65 ± 10
VPS66	Vacuolar trafficking	−	482 ± 39	56 ± 23
VPS69	Vacuolar trafficking	−	585 ± 95	89 ± 37
VPS71	Vacuolar trafficking	−	394 ± 165	156 ± 96
CLASS C				
VPS16	HOPS complex	+/−	894 ± 181	71 ± 11
PEP3/VPS18	HOPS complex	−	1000 ± 178	125 ± 64
CLASS D				
VPS3	Vacuolar segregation	−	2862 ± 105	184 ± 16
PEP12	t-SNARE of the PVC	−	973 ± 39	98 ± 14
VPS9	GDP/GTP exchange factor	−	372 ± 105	95 ± 05
VPS19	Vesicular transport from Golgi to endosomes	−	536 ± 17	140 ± 06
VPS45	Activation of t-SNARES in vesicular transport from Golgi to endosomes	+	518 ± 116	72 ± 13
CLASS E				
DID2/FTI1	Endosomal coiled-coil protein	+/−	582 ± 257	127 ± 32
VPS60/MOS10	Endosomal coiled-coil protein	+/−	1082 ± 501	137 ± 38
HSE1	In complex with Vps27p	+	682 ± 64	185 ± 90
VPS27	Recognition of cargo at the MVE	−	1938 ± 985	132 ± 75
STP22/VPS23	ESCRT-I complex	−	627 ± 270	89 ± 52
VPS28	ESCRT-I complex	−	1118 ± 656	143 ± 50
SRN2/VPS37	ESCRT-I complex	−	764 ± 309	123 ± 13
SNF8/VPS22	ESCRT-II complex	−	973 ± 107	107 ± 42
VPS25	ESCRT-II complex	−	2098 ± 302	136 ± 04
VPS36	ESCRT-II complex	−	1164 ± 129	136 ± 09
VPS20	ESCRT-III complex	−	973 ± 64	105 ± 46
SNF7/VPS32	ESCRT-III complex	−	964 ± 77	88 ± 48
DID4/VPS2	ESCRT-III complex	−	2863 ± 425	137 ± 69
VPS24	ESCRT-III complex	−	2682 ± 119	149 ± 14
VPS4	Disassembly of complexes at the MVE	−	1902 ± 720	135 ± 36
BRO1/VPS31	Doa4p recruitment to MVE	−	2787 ± 437	187 ± 25
NHX1	Na+/H+ antiporter	−	553 ± 90	92 ± 12
CLASS F				
PEP8/VPS26	Retromer complex	+	427 ± 116	99 ± 31
VPS65	Cytoskeleton organization	−	521 ± 45	75 ± 01
OTHERS				
FAB1	PI(3)P-5 kinase; MVEs function	+	100 ± 13	84 ± 19
DEF1/VID31	Vacuolar sorting	+	265 ± 20	70 ± 30
DOA4	Deubiquitination of cargo at the MVEs	−	2560 ± 132	119 ± 08
TUL1	Ubiquitination of misfolded proteins targeted to vacuole for degradation	+	309 ± 51	113 ± 16
PIB1	Ub ligase, endosomal/vacuolar resident	+	100 ± 13	127 ± 22

[a] ADCB phenotype is expressed as in Table 3.

[b] Gap1p activity in each mutant is expressed as a percentage of the [^{14}C]citrulline uptake rate of wild type cells growing in minimal urea liquid medium. [^{14}C]arginine uptake is also shown as a control. The SD of four independent experiments is shown.

Gap1p activity of more than 20-fold after 20 min that was equivalent in wild-type and in the class E *vps* mutants. As a control to demonstrate that the decline in Gap1p activity was at least in part due to endocytosis, we showed that the endocytic mutant *end3*Δ did not exhibit a significant reduction in Gap1p activity after the addition of glutamate (Figure 3C).

These data indicate that, although class E *vps* mutants caused increased traffic of Gap1p to the plasma membrane, these mutants can respond normally to high external and internal amino acid concentrations by redirecting Gap1p away from the plasma membrane to the vacuolar targeting pathway. This behavior clearly distinguishes class E vps mutants from mutations that affect Gap1p ubiquitination, such as a *bul1*Δ *bul2*Δ double mutant, because the latter not only cause an increase in Gap1p activity, but also render Gap1p sorting insensitive to the effect of amino acids.

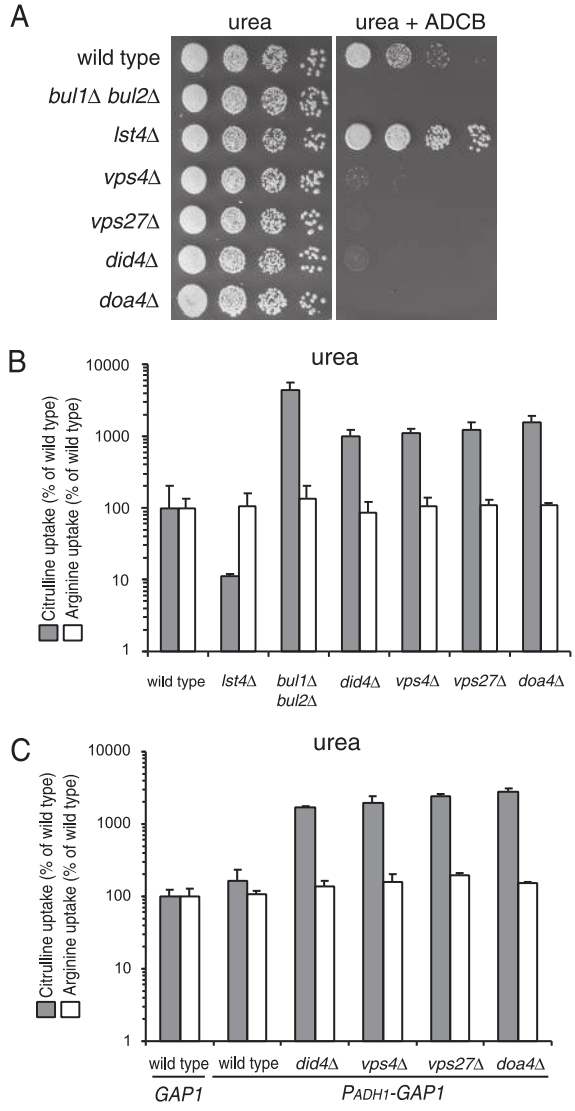

Figure 1. Null mutations in class E *vps* genes cause increased activity of Gap1p. (A) Wild-type (CKY835), *lst4*Δ (CKY695), *bul1*Δ *bul2*Δ (CKY698), *did4*Δ (CKY839), *vps4*Δ (CKY836), *vps27*Δ (CKY837), and *doa4*Δ (CKY838) strains were spotted as serial dilutions onto minimal urea medium, with or without 7 mg/l of ADCB. (B) The same strains were grown in liquid minimal urea medium and assayed for [^{14}C]citrulline and [^{14}C]arginine uptake. (C) Wild-type (CKY835) and strains carrying a genomic P_{ADH1}-*GAP1* replacement of the endogenous *GAP1* gene (CKY833), combined with *did4*Δ (CKY840), *vps4*Δ (CKY841), *vps27*Δ (CKY842), and *doa4*Δ (CKY843) mutations, were assayed for [^{14}C]citrulline and [^{14}C]arginine uptake. The data are expressed as a percentage of the rate of uptake for the wild-type strain and represent the mean for at least four independent experiments. Error bars, 1 SD.

Gap1p Traffic to the Plasma Membrane in a Class E vps Mutant Is Blocked by an LST4 *Mutation*

Mutations in the gene *LST4* dramatically reduce the activity of Gap1p because they cause constitutive sorting of Gap1p to the vacuole, regardless of the nitrogen source in the growth medium (Roberg *et al.,* 1997b). Nevertheless, the *lst4*Δ phenotype can be completely suppressed by a *bul1*Δ *bul2*Δ double mutant, suggesting that Gap1p encounters the sorting step specified by Bul1p and Bul2p before the step that depends on Lst4p (Helliwell *et al.,* 2001). In contrast to the behavior shown by the triple mutant *bul1*Δ *bul2*Δ *lst4*Δ, a simultaneous mutation of the gene *LST4* completely rescued growth of the *bro1*Δ, *vps4*Δ, *vps27*Δ, and *did4*Δ mutants on plates of minimal ammonia (Figure 4A) or urea (our unpublished data) medium containing 7 mg/l of ADCB. Uptake assays to measure Gap1p activity levels were consistent with the sensitivity to ADCB. Double mutants, *lst4*Δ *vps4*Δ, *lst4*Δ *vps27*Δ, and *lst4*Δ *did4*Δ, all had ~5% of the Gap1p activity as the corresponding single class E mutant (Figure 4B). Null double mutants with *lst4*Δ for the remaining class E genes showed similar reductions of Gap1p activity except for an *lst4*Δ *bro1*Δ double mutant, which exhibited 20% of the activity as a *bro1*Δ single mutant.

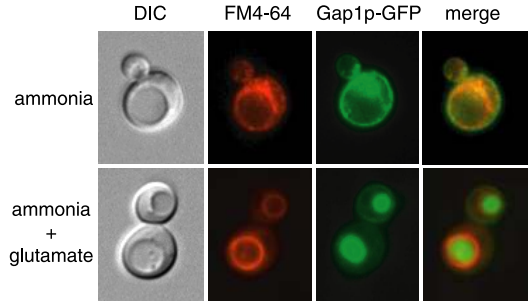

Figure 2. Gap1p is sorted into the vacuolar lumen. A wild-type strain expressing a genomic GFP-tagged version of *GAP1* (CKY834) was grown to exponential phase in minimal ammonia medium. Glutamate was added to a final concentration of 3 mM, and cells were incubated for an additional hour. Cells were then labeled with the vacuolar membrane staining dye FM4-64 for 30 min, followed by a 60-min chase before microscopy. Cells were imaged using a UV fluorescence microscope with a GFP filter (GFP), a rhodamine filter (FM4-64), and by Nomarski optics (DIC).

The subcellular localization of Gap1p-GFP in wild-type cells grown in ammonia medium typically showed the majority of Gap1p-GFP located at the cell surface and a minor intracellular signal corresponding to internally stored pools (Figures 2 and 5A). By contrast, Gap1p-GFP in the *lst4*Δ mutant was localized within the vacuolar lumen and to punctate structures surrounding the vacuole. Null mutations in the class E genes, *VPS4*, *VPS27*, *DID4*, and *BRO1*, showed Gap1p-GFP predominantly located at the plasma membrane. Instead, the double mutants, *lst4*Δ *vps4*Δ, *lst4*Δ *vps27*Δ, and *lst4*Δ *did4*Δ, showed most of Gap1p-GFP contained in structures adjacent to the vacuole, which was visualized using DIC optics. Similar results were obtained for deletions in *VPS28*, *SNF8*, *VPS25*, *VPS36*, *VPS20*, *SNF7*, and *VPS24* (our unpublished data).

These data clearly distinguish the effect of Gap1p ubiquitination mutants (exemplified by *bul1*Δ *bul2*Δ) from class E *vps* mutants. Although both types of mutants exhibit a redistribution of Gap1p to the plasma membrane accompanied by greatly increased Gap1p permease activity, the class E *vps* mutants will respond to regulation by amino acids and *lst4*Δ mutations, whereas ubiquitination-defective mutants are not influenced by either. Overall, these results along with the previously demonstrated existence of an internal pool of Gap1p, even when cells are grown in poor nitrogen sources (Roberg *et al.,* 1997a; Helliwell *et al.,* 2001), suggest that Gap1p is continuously sorted through the MVE, but in mutants defective for MVE formation, the Gap1p that accumulates in this compartment is available to be returned to the plasma membrane by a recycling pathway that depends on *LST4* function and is regulated by amino acids.

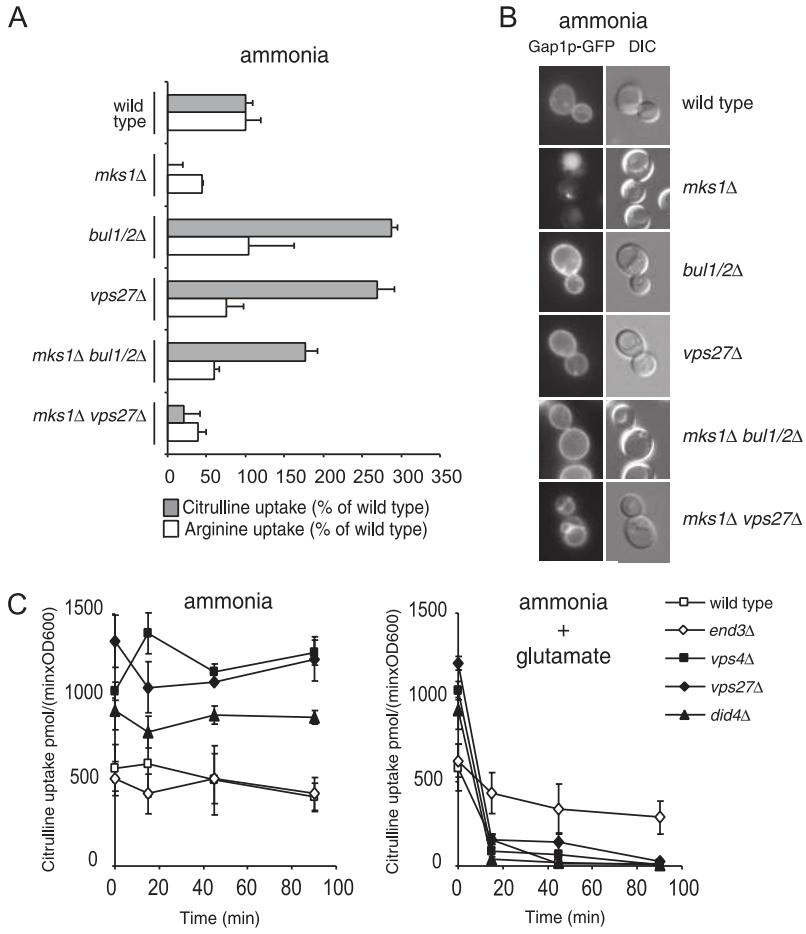

Figure 3. Inactivation of Gap1p activity by amino acids occurs in the class E *vps* mutants but not in mutants impaired for Gap1p ubiquitination. (A) [^{14}C]citrulline and [^{14}C]arginine uptake as assayed in a mutant with increased levels of catabolic amino acids, *mks1*Δ (CKY758), combined with the mutant background defective in Gap1p polyubiquitination, *bul1*Δ *bul2*Δ (*mks1*Δ *bul1*Δ *bul2*Δ*;* CKY923) or the mutant class E background, *vps27*Δ (*mks1*Δ *vps27*Δ*;* CKY924). Activities for the wild-type strain (CKY835) and the mutant controls *bul1*Δ *bul2*Δ (CKY698) and *vps27*Δ (CKY837) grown in parallel are provided for comparison. The cell cultures were grown in minimal ammonia medium. Averaged data are expressed as in Figure 1. (B) Gap1p-GFP localization is shown in cells from the mutants *mks1*Δ (CKY867), *mks1*Δ *bul1*Δ *bul2*Δ (CKY926), and *mks1*Δ *vps27*Δ (CKY927), grown in minimal medium with ammonia as a nitrogen source. Gap1p-GFP images of the wild-type strain (CKY834), the mutant controls *bul1*Δ *bul2*Δ (CKY925), and *vps27*Δ (CKY851), grown identically, are shown for comparison. (C) A [^{14}C]citrulline uptake time course from the following strains: wild-type (CKY835; □), *end3*Δ (CKY934; ◇), *did4*Δ (CKY839; ▲), *vps4*Δ (CKY836; ■), and *vps27*Δ (CKY837; ◆), growing in liquid minimal ammonia medium (left panel) or ammonia medium plus 3 mM glutamate, added when the strains were at OD_{600} of 0.2/ml (right panel), is shown. These graphics show the averaged data between three independent experiments.

Different Subsets of MVE Proteins Have Different Effects on the Retention of Gap1p in the MVE

Our results above indicate that a specific subset of class E *vps* mutants growing in the absence of high amino acid concentrations fail to retain Gap1p in the MVE. Although all class E *vps* mutations showed increased levels of Gap1p activity under these conditions, some of the mutants had more subtle effects on Gap1p. Mutants such as *vps60*Δ and *hse1*Δ were slightly less sensitive to low concentrations of ADCB (our unpublished data). Similarly, *did2*Δ, *hse1*Δ, *vps23*Δ, and *vps37*Δ, had only 5- to 7-fold increased levels of Gap1p activity when grown in urea as a nitrogen source (Table 4), which is about half of the effect shown by the mutations described above.

We examined the subcellular localization of Gap1p-GFP in this different subgroup using *did2*Δ, *hse1*Δ, *vps23*Δ, *vps37*Δ, or *vps60*Δ null mutant strains. These single mutant strains growing in ammonia displayed a pattern of Gap1p-GFP localization similar to that of a *vps27*Δ *lst4*Δ double mutant (compare Figure 5, A and B), with most of the Gap1p-GFP being located intracellularly. Confocal microscopy of these cells revealed that the diffuse pattern of localization of Gap1p-GFP was the result of some Gap1p-GFP in punctate structures adjacent to the vacuole as well as in the vacuolar membrane (our unpublished data). Apparently mutations in this subset of ESCRT genes do not allow Gap1p to exit the MVE efficiently. The differences among ESCRT mutants with respect to their effect on Gap1p do not strictly correlate with the known subdivisions of these proteins into different complexes; however, most of the mutants that allow efficient cycling of Gap1p to the plasma membrane are in ESCRT complex II and III.

A Preexisting Pool of Gap1p Can Cycle from the MVE to the Plasma Membrane

To demonstrate directly the existence of a pathway for cycling of existing Gap1p from the MVE to the plasma membrane, we accumulated Gap1p in the class E compartment in a *vps4*Δ mutant grown on glutamate and then transferred the cells to amino acid–free medium. As expected, the *vps4*Δ mutant grown on glutamate exhibited low levels of Gap1p activity, but when these cells were transferred to urea medium Gap1p activity increased rapidly (Figure 6A). The initial rise in activity experienced by the *vps4*Δ mutant did not depend on newly synthesized permease because the early phase of induction of activity was not blocked by addition of 1.5 μg/ml cycloheximide. This concentration of cycloheximide was chosen as the minimum necessary to inhibit translation completely as assayed by incorporation of radiolabeled methionine into newly translated proteins (Figure 6B; Roberg *et al.,* 1997a). In contrast, activity did not increase substantially in an *lst4*Δ *vps4*Δ double mutant (that was not treated with cycloheximide), showing that Gap1p cycling to the plasma membrane does depend on Lst4p activity (Figure 6A). An immunoblot control (Figure 6C) shows that each of the cultures contained similar amounts of Gap1p protein, indicating that the differences in activity were not due to Gap1p degradation. In a parallel localization experiment, Gap1p-GFP could be seen to partially redistribute from the endosome to the plasma membrane in a *vps4*Δ

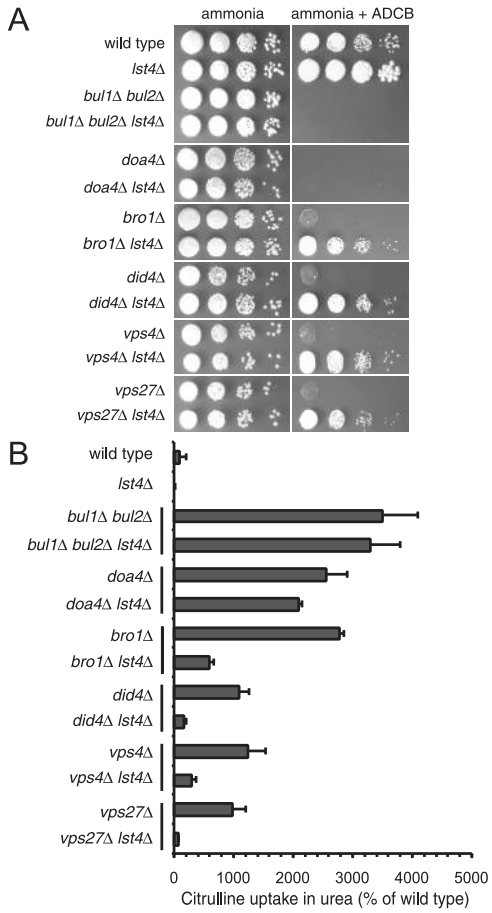

Figure 4. The *lst4*Δ mutation has a similar effect on Gap1p trafficking as glutamate and high amino acid concentrations. The strains *doa4*Δ (CKY838) and *lst4*Δ *doa4*Δ (CKY847), *bro1*Δ (CKY935) and *lst4*Δ *bro1*Δ (CKY936), *did4*Δ (CKY839) and *lst4*Δ *did4*Δ (CKY844), *vps4*Δ (CKY836) and *lst4*Δ *vps4*Δ (CKY845), *vps27*Δ (CKY837) and *lst4*Δ *vps27*Δ (CKY846), were spotted as serial dilutions onto minimal ammonia medium, with or without a sub-LC of ADCB (7 mg/l). As control strains, a wild-type strain (CKY835) and the mutants *lst4*Δ (CKY695), *bul1*Δ *bul2*Δ (CKY698), and *lst4*Δ *bul1*Δ *bul2*Δ (CKY699) grown in identical conditions, are shown in the top panel. (B) The same strains growing in minimal urea medium were assayed for [^{14}C]citrulline uptake. Averaged data are expressed as in Figure 1.

mutant after transfer from glutamate to urea medium. However, most of the Gap1p-GFP remained in the class E compartment in an *lst4*Δ *vps4*Δ double mutant under the same conditions (Figure 6D).

Interestingly, a different pattern of modified species of Gap1p can be detected by Western blot between the mutants *vps4*Δ and *lst4*Δ *vps4*Δ (Figure 6C). The mutant *lst4*Δ *vps4*Δ shows accumulation of several high-molecular-weight species containing Gap1p that are absent in protein extracts from *vps4*Δ. A wild-type strain shows a pattern similar to that observed in the *lst4*Δ *vps4*Δ, and these species are absent in a mutant strain carrying an allele of *GAP1* with the two lysine acceptor sites for ubiquitination mutated to arginine (*gap1*^{K9R,K16R}; Soetens *et al.*, 2001), suggesting that these species correspond to ubiquitinated forms of Gap1p (Risinger and Kaiser, personal communication). A lower level of polyubiquitinated species of Gap1p has also been observed in other class E *vps* mutant strains grown in similar conditions (our unpublished data). This phenomenon may be related to a particular form of the endosomally localized Gap1p that accumulates when the MVE pathway is blocked.

Gap1p Recycling Does Not Depend on Other Known Pathways for Recycling Proteins from the Endosome to Golgi Compartments

Three different protein complexes have been identified for their role in the recycling of different subsets of proteins from the endosome to the Golgi. The vps fifty three (VFT)/Golgi-associated retrograde protein (GARP) complex consists of four subunits (Vps51p–Vps54p) and is required in association with the Rab Ypt6p for the retrograde transport of Golgi resident proteins from the endosome to the Golgi (Conibear and Stevens, 2000; Siniossoglou and Pelham, 2002). A second complex, known as the retromer complex, is necessary for recycling of Vps10p and is composed of Vps35p, Vps29p, and Vps26p and the Vps5p–Vps17p sorting nexin dimer (Reddy and Seaman, 2001; and reviewed by Seaman, 2005). A third multisubunit tethering complex with a recently discovered role in the recycling of the uracil permease Fur4p (Bugnicourt *et al.*, 2004) that was first identified as being involved in the docking and fusion of vacuolar and/or endosomal membranes is the class C Vps/homotypic fusion and vacuole protein sorting (HOPS) complex (reviewed by Wickner, 2002; Whyte and Munro, 2002). Proteins forming this complex include Pep3/Vps18p, Pep5/Vps11p, Vps16p, Vps33p, Vam3p, and Ypt7 (Raymond *et al.*, 1992, Whyte and Munro, 2002). Notably, a requirement for Vam3p in the recycling of Gap1p has been suggested (Nikko *et al.*, 2003).

If any of these complexes were necessary for Gap1p trafficking from the MVE to the plasma membrane, the corresponding mutants would be expected to exhibit an effect on Gap1p trafficking similar to *lst4*Δ. However, none of the mutations in the three known recycling complexes exhibited a significant decrease in Gap1p activity (Tables 3 and 4; Figure 7). Moreover, some of the class C Vps mutant strains, even showed increased levels of Gap1p activity that closely resembled to those observed for class E Vps mutations.

As an explicit test of the role of known recycling complexes in Gap1p recycling, we constructed double mutants with *vps4*Δ and determined the effect on Gap1p activity (Figure 7). Retromer mutations did not cause a significant reduction of the increased levels of Gap1p activity observed in a *vps4*Δ mutant. Some mutations such as *vps26*Δ actually increased the level of Gap1p activity. VFT/GARP complex mutants combined with *vps4*Δ caused a modest decrease in Gap1p activity relative to a *vps4*Δ single mutation, but the effect was much less than for that of an *lst4*Δ mutation and likely does not indicate a direct effect on Gap1p trafficking to the plasma membrane. Vps/HOPS complex mutants had a heterogeneous effect in the levels of Gap1p activity in a *vps4*Δ genetic background: compared with a *vps4*Δ single mutant, double mutations with *vps16*Δ or *vps33*Δ modestly decreased Gap1p activity, whereas double mutants with *vam3*Δ or *pep3/vps18*Δ either did not alter Gap1p activity or caused increased activity.

Specific Dependence of Gap1p Recycling on LST4 *and* LST7 *Genes*

We were interested in whether the genes we have identified that do have a significant effect on Gap1p trafficking from the MVE to the plasma membrane affected other recycling processes. We therefore examined *LST4* and *LST7*, two of the genes we have isolated that have the greatest effect on Gap1p trafficking to the plasma membrane (Roberg *et al.*, 1997b), for their effects on a variety of trafficking events.

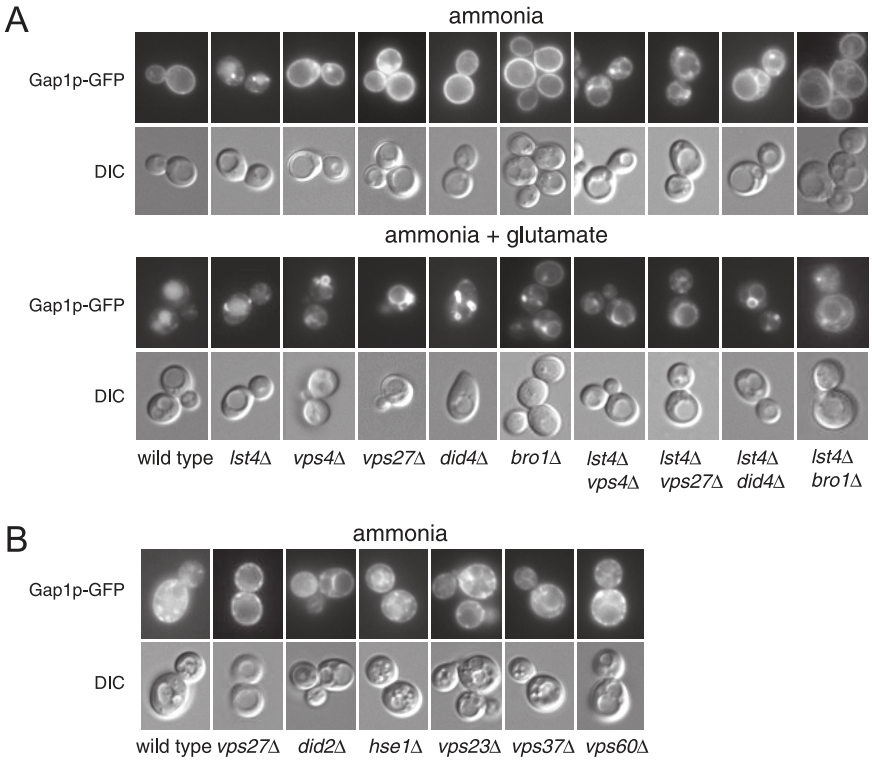

Figure 5. Class E *VPS* mutants accumulate Gap1p-GFP in endosomal and perivacuolar membranes in the presence of glutamate or an *lst4*Δ mutation. (A) Fluorescence microscopy images of wild-type cells (CKY834) and the mutants *lst4*Δ (CKY848), *vps4*Δ (CKY850), *vps27*Δ (CKY851), *did4*Δ (CKY849), *bro1*Δ (CKY937), *lst4*Δ *vps4*Δ (CKY854), *lst4*Δ *vps27*Δ (CKY855; leucine auxotrophy covered by the *CEN-LEU2* plasmid pRS415), *lst4*Δ *did4*Δ (CKY853), *lst4*Δ *bro1*Δ (CKY938), expressing genomic GFP-tagged Gap1p and exponentially growing in minimal ammonia medium, or incubated for 1 h in the presence of 3 mM glutamate before imaging. (B) A subset of class E *vps* mutations causes accumulation of Gap1p-GFP in endosomal and perivacuolar membranes in the absence of high concentrations of amino acids. Cells from wild-type strain (CKY835) and the mutants *vps27*Δ (CKY837), *did2*Δ (CKY857), *hse1*Δ (CKY858), *vps23*Δ (CKY859), *vps37*Δ (CKY860), and *vps60*Δ (CKY861), expressing Gap1p-GFP from a centromeric plasmid (p*GAP1-GFP*) and exponentially growing in minimal ammonia medium were imaged by fluorescence microscopy.

Both *lst4*Δ and *lst7*Δ caused a greater than 20-fold decrease in Gap1p activity in the context of a *vps4*Δ genetic background (Figure 8A). This decreased Gap1p activity did not correspond to a decrease in *GAP1* transcription (Figure 8B) and most likely resulted from a failure of Gap1p to be transported efficiently from the class E compartment to the plasma membrane (Figure 8C). However, neither *lst4*Δ nor *lst7*Δ appeared to have an effect on Vps10p cycling between the Golgi and endosome because these mutants did not cause an increase in secretion of pro-CPY into the extracellular medium (Figure 8D). Moreover, neither *lst4*Δ nor *lst7*Δ had an effect on FM4-64 recycling from an endosomal com-

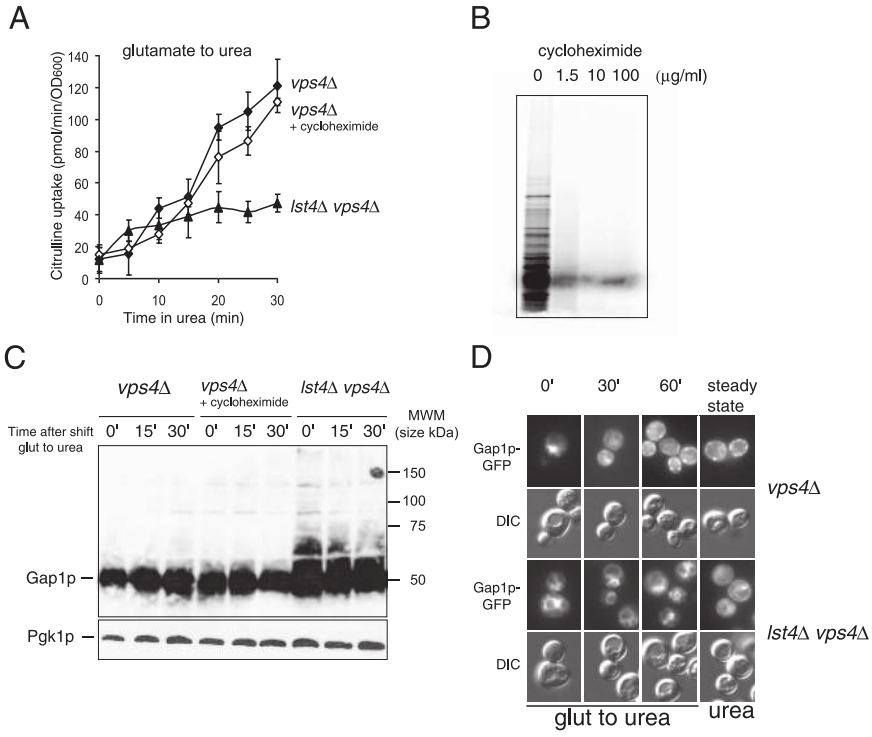

Figure 6. Gap1p accumulated in the prevacuolar compartment of a class E *vps* mutant can recycle to the plasma membrane. (A) The strains *vps4*Δ (CKY836) and *vps4*Δ *lst4*Δ (CKY845), grown in minimal glutamate medium, were transferred to minimal urea medium and immediately assayed for [^{14}C]citrulline uptake at different times after the shift. Activity time courses are represented as filled diamonds (*vps4*Δ) or filled triangles (*vps4*Δ *lst4*Δ). The strain *vps4*Δ was also assayed in the presence of 1.5 μg/ml cycloheximide in the urea-containing medium before shift, to inhibit translation of newly synthesized Gap1p (◇). (B) The effect of cycloheximide (0, 1.5, 10, and 100 μg/ml) on bulk translation was assayed by pulse labeling *vps4*Δ (CKY836) on minimal glutamate medium with [^{35}S]methionine. (C) Protein extracts taken at the same time-point periods and using the same strains and conditions as in A, were subject to SDS-PAGE and Western blotting with Gap1p antibody. As a loading control, Pgk1p levels are shown (bottom blot). Each lane contains an extract from the same number of cells. (D) The strains *vps4*Δ (CKY850) and *lst4*Δ *vps4*Δ (CKY854) were monitored for Gap1p-GFP localization at different periods of time after being shifted from minimal glutamate medium to urea medium. For comparison, images of the same strains steadily growing in urea are also shown.

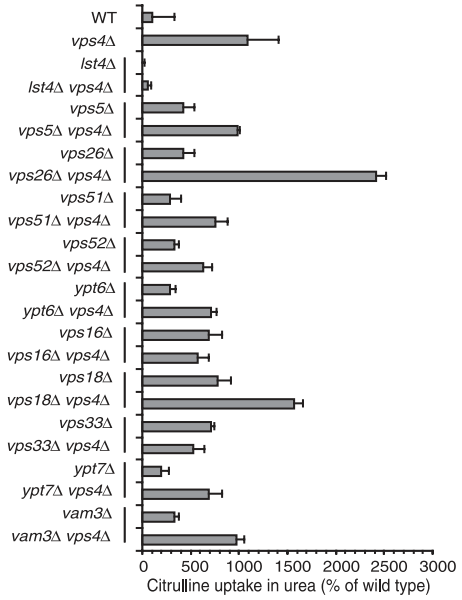

Figure 7. Recycling of Gap1p is not severely affected by defects in pathways involved in the recycling of proteins from the MVE. The following strains were grown in liquid minimal urea medium and assayed for [^{14}C]citrulline uptake: wild type (CKY835), *lst4*Δ (CKY695), *vps4*Δ (CKY836), *lst4*Δ *vps4*Δ (CKY845), *vps5*Δ (Y01845), *vps5*Δ *vps4*Δ (CKY995), *vps26*Δ (Y01370), *vps26*Δ *vps4*Δ (CKY996), *vps51*Δ (Y05091), *vps51*Δ *vps4*Δ (CKY997), *vps52*Δ (Y04318), *vps52*Δ *vps4*Δ (CKY998), *vps16*Δ (Y02783), *vps16*Δ *vps4*Δ (CKY999), *vps18*Δ (Y04105), *vps18*Δ *vps4*Δ (CKY1000), *ypt6*Δ (Y05171), *ypt6*Δ *vps4*Δ (CKY1001), *ypt7*Δ (Y00575), *ypt7*Δ *vps4*Δ (CKY1002), *vam3*Δ (Y02362), *vam3*Δ *vps4*Δ (CKY1003), *vps33*Δ (Y05305), *vps33*Δ *vps4*Δ (CK1004). Measurements of Gap1p activity are expressed as in Figure 1. Single mutant strains in the BY4741 background (EUROSCARF deletion strains), and some of the double mutant strains were transformed with the centromeric plasmid p*CEN-HIS3-LEU2-MET15* (pCK283) to eliminate auxotrophic requirements for amino acids.

partment back to the plasma membrane (Figure 8, E and F). Taken together these results indicate that Gap1p has a discrete set of genetic requirements for trafficking from the MVE to the plasma membrane that does not appear to overlap with known endosomal or MVE recycling pathways.

Intracellular Accumulation of Gap1p Does Not Depend on Endocytosis

As shown above, a class E *vps* mutant requires relatively low amino acid levels and functional Lst4p to give rise to increased levels of Gap1p at the plasma membrane. Accordingly, we hypothesized that Lst4p is required for trafficking of Gap1p from the class E compartment to the plasma membrane (probably via the Golgi) under conditions of low intracellular amino acids. However, the possibility remained that Lst4p could negatively regulate Gap1p endocytosis and that amino acids such as glutamate could stimulate endocytosis, such that the rate of Gap1p endocytosis was greatly increased in an *lst4*Δ mutant. One way to resolve these possibilities is to examine the effect of a mutation known to block Gap1p endocytosis. *END3* encodes a component of general endocytic vesicles and *end3*Δ mutants completely block endocytosis of a variety of membrane proteins, including Gap1p (Benedetti *et al.,* 1994; Nikko *et al.,* 2003; Figure 3C). If an *lst4*Δ mutation caused an increased rate of Gap1p endocytosis, then it should be possible to reverse the effect of an *lst4*Δ mutant by blocking endocytosis with *end3*Δ. We examined Gap1p-GFP localization in *end3*Δ and *lst4*Δ single mutants and *end3*Δ *lst4*Δ double mutant strains (Figure 9A). A block in Gap1p-GFP endocytosis was evident in *end3*Δ mutants since Gap1p-GFP remained at the plasma membrane for more than 30 min when grown on ammonia, after the addition of glutamate, whereas the wild-type strain showed complete redistribution of Gap1p-GFP to the vacuole under the same conditions. When *end3*Δ mutant cells were grown continuously on glutamate, Gap1p-GFP accumulated in the vacuole, and no signal appeared at the plasma membrane, indicating that upon continued exposure to glutamate vacuolar sorting of Gap1p occurs through a pathway that does not involve previous sorting to the plasma membrane (as previously demonstrated by Roberg *et al.,* 1997a). Similarly, in an *lst4*Δ mutant most Gap1p-GFP is transported to the vacuole by a pathway that bypasses the plasma membrane because most Gap1p-GFP was delivered to the vacuole in an *end3*Δ *lst4*Δ double mutant grown on ammonia. Some of the *end3*Δ *lst4*Δ mutant cells showed a small fraction of Gap1p-GFP at the cell surface consistent with the expectation that the small fraction of Gap1p-GFP delivered to the cell surface in an *lst4*Δ mutant would accumulate in that location in an *end3*Δ mutant. The amount of Gap1p-GFP at the cell surface in an *end3*Δ *lst4*Δ, quantified by Gap1p activity assay, was similar to the low activity in an *lst4*Δ mutant (Figure 9B), in accordance with previous observations made by Helliwell *et al.* (2001). These observations rule out the possibility that the effect of *lst4*Δ or growth on glutamate act to decrease Gap1p at the plasma membrane by greatly increasing the rate of endocytosis.

Vacuolar Sorting of Gap1p Can Occur Independently of GGA Function

GGA (Golgi-associated, γ-adaptin homologues, ARF-binding) proteins have a well-characterized role in the recycling of sorting receptors of vacuolar/lysosomal hydrolases from endosomes to the TGN (reviewed by Bonifacino, 2004). Recent work has shown that GGA proteins can bind ubiquitin directly through their GAT domains and that defects in GGA function result in defective vacuolar sorting of Gap1p (Bilodeau *et al.,* 2004; Scott *et al.,* 2004). These observations suggest that GGA proteins may be responsible for sorting ubiquitinated Gap1p from the TGN to endosomes, although a direct binding of GGA proteins to ubiquitinated Gap1p has not been demonstrated. We wanted to ascertain whether the constitutive vacuolar sorting occurring in a null mutant *lst4*Δ strain is impaired when both *GGA* genes from *Saccharomyces*, *GGA1* and *GGA2*, are simultaneously deleted. With this aim we decided to monitor Gap1p-GFP localization in the double mutant *gga1*Δ *gga2*Δ and the triple mutant *gga1*Δ *gga2*Δ *lst4*Δ. As shown in Figure 10, when cells from the double mutant *gga1*Δ *gga2*Δ growing in ammonia are switched to medium with glutamate, cells show a significant defect in the ability to sort Gap1p to the vacuole. This is in accordance with the previous observations reported by Scott *et al.* (2004). However, the triple mutant *gga1*Δ *gga2*Δ *lst4*Δ did not show any defect associated with the lack of GGA function and instead behaved as an *lst4*Δ mutant, showing constitutive sorting of Gap1p to the vacuole independent from the nitrogen source. In contrast, an *lst4*Δ *pep12*Δ double mutant showed Gap1p-GFP associated with small punctae that probably correspond with multiple small vesicles unable to fuse/form an endosome (Figure 10). This latter result served as a control to show that a known block in Golgi-to-MVE traffic impairs constitutive sorting of Gap1p to the vacuole in an *lst4*Δ (*PEP12* gene encodes a t-SNARE of the

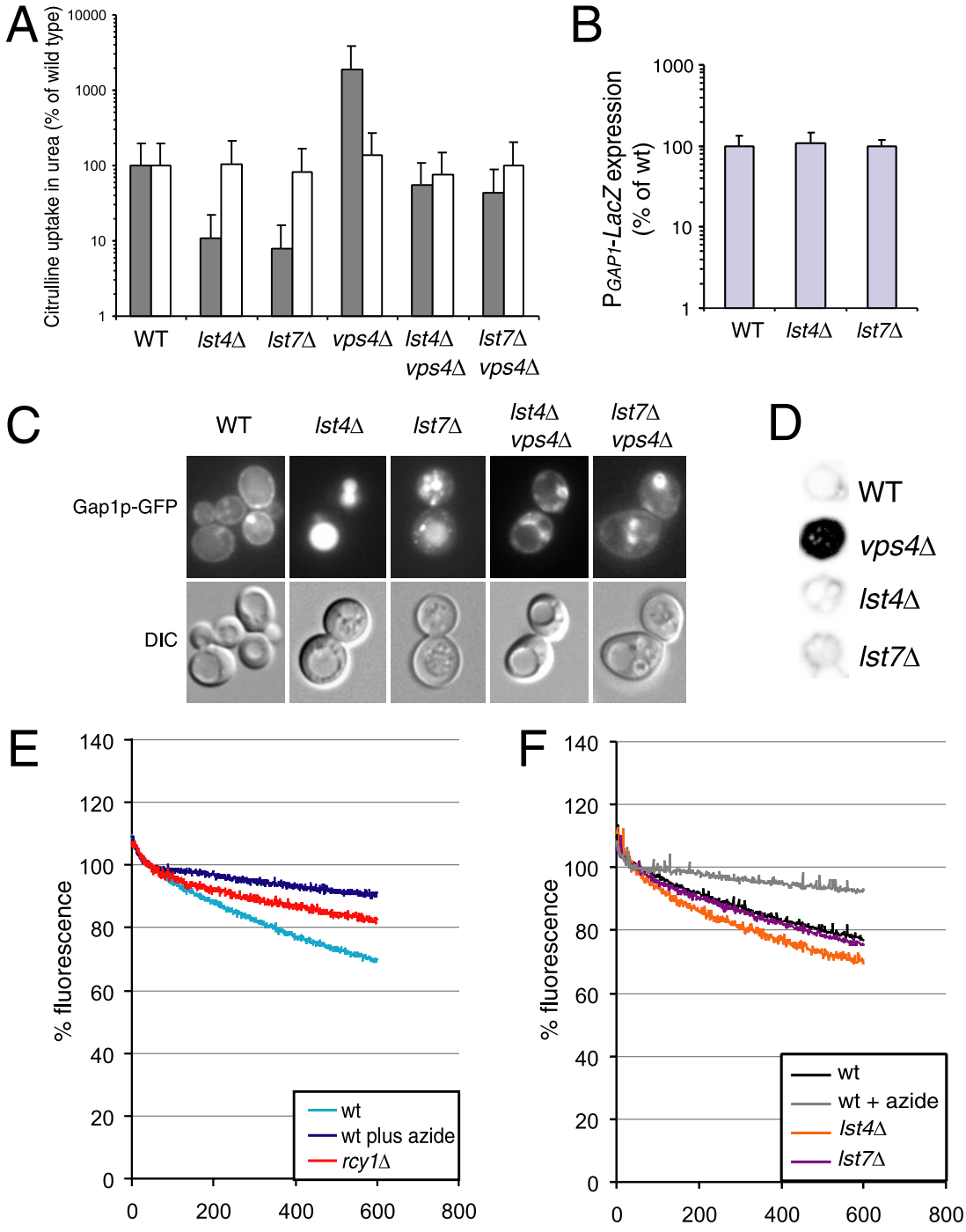

Figure 8. *LST4* and *LST7* are required specifically for Gap1p sorting. (A) *lst4*Δ and *lst7*Δ mutations interfere with Gap1p distribution to the plasma membrane caused by a *vps4*Δ mutation. The following strains were grown in minimal urea medium and assayed for uptake of [^{14}C]citrulline and [^{14}C]arginine: wild type (CKY835), *lst4*Δ (CKY695), *lst7*Δ (CKY994), *vps4*Δ (CKY836), *lst4*Δ *vps4*Δ (CKY845), and *lst7*Δ *vps4*Δ (CKY1005). (B) The decrease in Gap1p activity caused by *lst4*Δ and *lst7*Δ mutations is not a transcriptional effect. Wild type (CKY835), *lst4*Δ (CKY695), and *lst7*Δ (CKY994) strains were transformed with the P_{GAP1}-*LacZ* (pMS29) plasmid and assayed for β-galactosidase activity after growth in minimal urea medium. (C) *lst4*Δ and *lst7*Δ mutations cause constitutive sorting of Gap1p to the vacuole and block its recycling caused by a *vps4*Δ mutation. Cells from wild-type strain (CKY835) and the mutants *lst4*Δ (CKY695), *lst7*Δ (CKY994), *lst4*Δ *vps4*Δ (CKY845), and *lst7*Δ *vps4*Δ (CKY1005), expressing Gap1p-GFP from a centromeric plasmid (p*GAP1-GFP*) and exponentially growing in minimal ammonia medium were visualized by fluorescence microscopy. (D) Wild-type (CKY835) *vps4*Δ (CKY836), *lst4*Δ (CKY695), and *lst7*Δ (CKY994) were spotted on a nitrocellulose membrane on YPD plates (an equivalent to 0.5 OD_{600} of cells/spot) and after 16 h at 30°C secreted CPY was detected using monoclonal anti-CPY (Molecular Probes). (E and F) *lst4*Δ and *lst7*Δ mutations do not interfere with recycling of FM4-64. (E) The wild-type strain BY4741 was assayed for the ability to recycle the fluorescent membrane dye FM4–64 as explained in *Materials and Methods*. Fluorescence was measured every second for 10 min on a spectrofluorometer and the graphic represents the average of three independent experiments. As a negative control the same strain was treated with 10 mM NaN_3 to block vesicular trafficking, and as a positive control the mutant strain from identical genetic background, *rcy1*Δ (Y01221) was also assayed. (F) The same experiment as in E was carried out in parallel in the wild-type (CKY835), *lst4*Δ (CKY695), and *lst7*Δ (CKY994) strains.

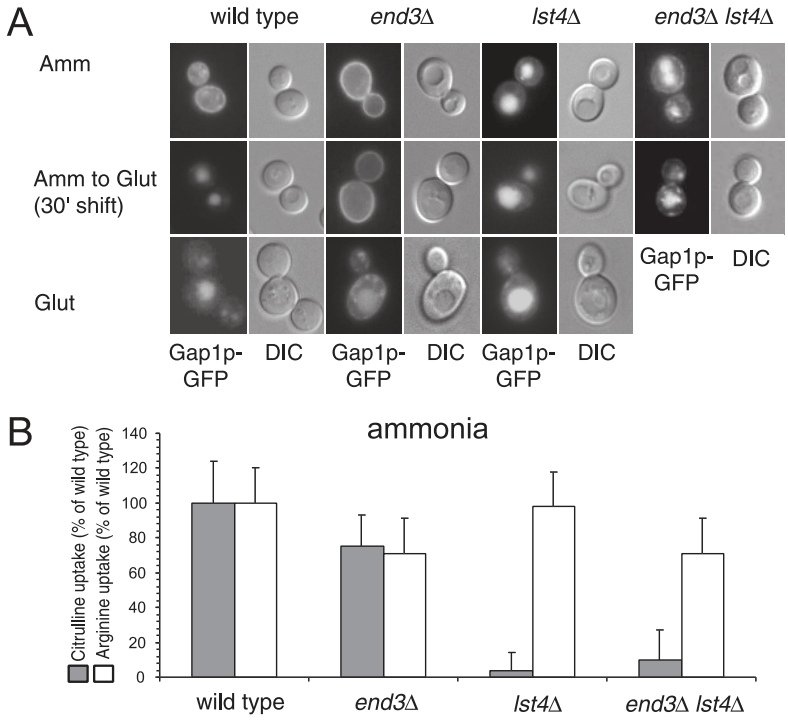

Figure 9. A *lst4*Δ mutation or growth on glutamate causes redistribution of Gap1p independently of endocytosis. Fluorescence microscopy images from cells of the wild-type (CKY834) strain, the mutant *lst4*Δ (CKY848), and the mutants impaired in endocytosis *end3*Δ (CKY874), and *end3*Δ *lst4*Δ (CKY875), expressing genomic GFP-tagged Gap1p, are shown. Cells were continuously grown to exponential phase in minimal medium with ammonia (top panel) or glutamate (bottom panel) as the only nitrogen source. Images of cells taken 30 min after the addition of glutamate 3 mM to induce endocytosis of Gap1p-GFP are also shown (middle panel). (B) The same strains were grown in liquid minimal ammonia medium and assayed for [^{14}C]citrulline and [^{14}C]arginine uptake, and the data were averaged as in Figure 1.

PVC required for the fusion with the endosome of vesicles trafficking toward the vacuolar sorting pathway; Becherer *et al.*, 1996) and established that whatever effect loss of *GGA* gene function may have on Gap1p sorting in the Golgi and endosomal compartments, it is neither quantitatively or qualitatively similar to the effect of *PEP12* gene function.

Doa4p Is Necessary for Deubiquitination of Gap1p

Deletion of *DOA4*, which encodes a deubiquitinating enzyme (ubiquitin C-terminal hydrolase) produces an effect on Gap1p trafficking to the cell surface, much like that of mutations in the Rsp5p/Bul1p/Bul2p ubiquitin ligase complex (Springael *et al.*, 1999). In a *doa4*Δ mutant Gap1p-GFP was localized to the plasma membrane but did not respond to the addition of 3 mM glutamate, suggesting a lack of proper ubiquitination-directed vacuolar sorting of the permease (Figure 11A). This finding is consistent with that of previous studies showing that Doa4p-deficient cells have a depleted pool of free ubiquitin because of a failure to recycle free ubiquitin monomers from ubiquitinated proteins

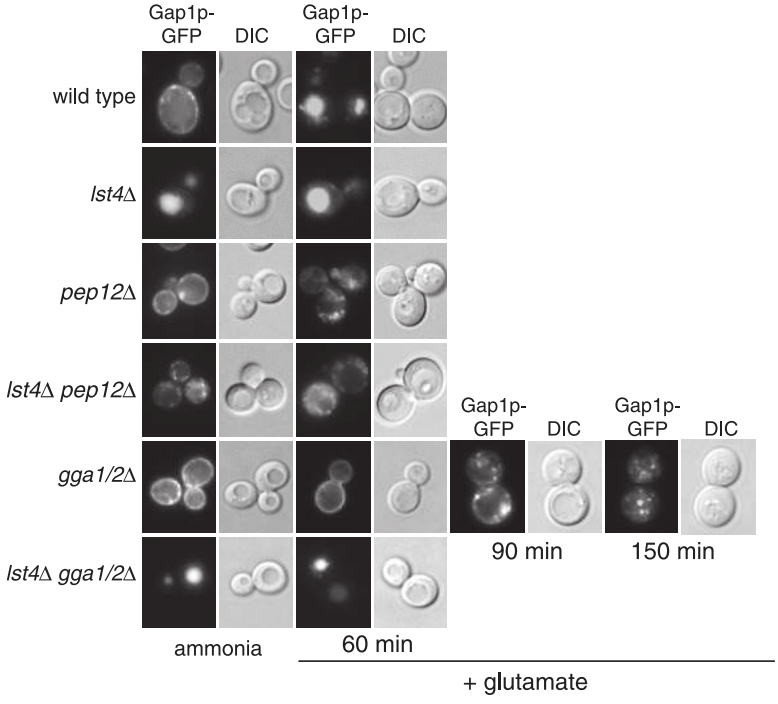

Figure 10. Constitutive vacuolar sorting of Gap1p in a *lst4*Δ mutant does not depend on GGA function. The following strains were transformed with the centromeric plasmid (p*GAP1-GFP*) and imaged by fluorescence microscopy to detect Gap1p-GFP localization: Wild-type (CKY835), *lst4*Δ (CKY695), *pep12*Δ (CKY694), *lst4*Δ *pep12*Δ (CKY1006), *gga1*Δ *gga2*Δ (CKY1007), and *lst4*Δ *gga1*Δ *gga2*Δ (CKY1008). Cells were continuously grown in ammonia or shifted from ammonia to glutamate.

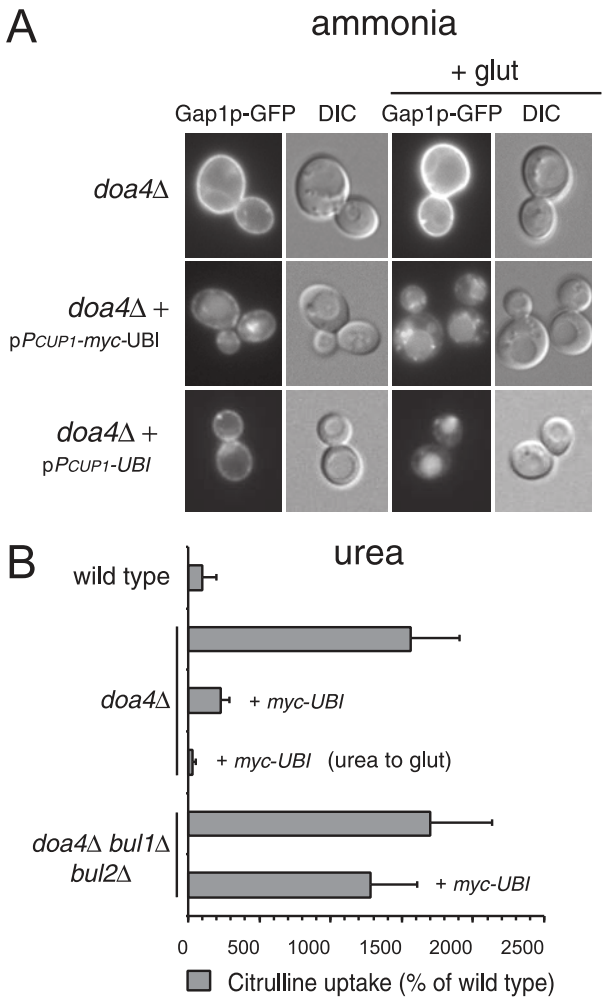

Figure 11. Overexpression of ubiquitin restores Gap1p vacuolar sorting in a *doa4*Δ mutant. (A) Gap1p-GFP localization in cells grown in minimal ammonia medium was monitored by fluorescence microscopy in a *doa4*Δ mutant (CKY852) alone or transformed with the P_{CUP1}-*myc-UBI* plasmid. Glutamate was added and cells were imaged after 30 min of incubation. The same experiment carried out by transformation with the P_{CUP1}-*UBI* plasmid is also shown. (B) Gap1p activity ([^{14}C]citrulline uptake rate) in strains constitutively expressing genomic HA-tagged Gap1p from the constitutive promoter *ADH1* was measured from cultures grown in minimal urea medium. The activity of a wild-type (CKY868) strain is compared with that of a *doa4*Δ mutant (CKY928) alone or transformed with the P_{CUP1}-*myc-UBI* plasmid. The ability of *doa4*Δ (CKY928) containing P_{CUP1}-*myc-UBI* compared with the inability of a *doa4*Δ *bul1*Δ *bul2*Δ (CKY930), carrying this same plasmid, to down-regulate Gap1p activity is also shown (shift from minimal urea medium to glutamate medium for 1 h). Averaged data are represented as in Figure 1.

(Swaminathan *et al.*, 1999). However, Doa4p may not only affect ubiquitination of newly synthesized Gap1p in the secretory pathway for vacuolar targeting but also affect deubiquitination of this permease at the MVE because it has already been shown that Doa4p associates with this compartment in order to deubiquitinate other proteins such as the uracil permease (Amerik *et al.*, 2000; Dupré and Haguenauer-Tsapis, 2001). To examine the effect of *doa4*Δ mutation on Gap1p deubiquitination, we used a strategy previously shown to compensate for the loss of free ubiquitin (caused by the defect in ubiquitin recycling) by overexpression of a functional N-terminal *myc* epitope-tagged ubiquitin (Ecker *et al.*, 1987; Ellison and Hochstrasser, 1991). A *doa4*Δ mutant strain carrying a multicopy plasmid (pP_{CUP1}-*myc-UBI*) was grown in the presence of 1 μM $CuSO_4$ to induce the expression of *myc*-Ub. Overexpression of *myc*-Ub could compensate for the effect of *doa4*Δ on Gap1p sorting as shown by the restoration of Gap1p-HA wild-type levels of activity (Figure 11B), and the ability of Gap1p-GFP to be rapidly relocated to the vacuole lumen when cells grown on ammonia (Figure 11A) or urea (Figure 11B) were transferred to glutamate medium. By contrast, the overexpression of *myc*-Ub was unable to restore wild-type levels of Gap1p activity in a *doa4*Δ *bul1*Δ *bul2*Δ strain (Figure 11B).

Gap1p-GFP was sorted into the vacuole lumen of *doa4*Δ cells overexpressing *myc*-Ubi. However, luminal sorting occurred with a lower efficiency than in a wild-type strain, with some of Gap1p-GFP accumulating at the vacuolar membrane and at adjacent punctate structures that may represent endosomes (Figure 11A). This partial defect in luminal sorting could be attributed to an effect of *myc*-tagged ubiquitin interfering with efficient targeting of Gap1p into luminal vesicles of the MVE, because parallel experiments with untagged ubiquitin (pP_{CUP1}-*UBI*) showed normal localization of Gap1p-GFP in a *doa4*Δ mutant (Figure 11A, bottom panel). Importantly, this result demonstrates that deubiquitination of Gap1p by Doa4p is not required for sorting of the permease in the intralumenal vesicles at the MVE.

To more thoroughly evaluate the possible role of Doa4p deubiquitination of Gap1p, we also detected ubiquitinated forms of the permease by immunoprecipitation followed by immunoblotting for *myc*-Ub. These experiments were carried out in strains expressing Gap1p-HA from the constitutive promoter *ADH1* to avoid any possible variability in *GAP1* expression and a deletion of *PEP4* to minimize the possibility of degradation of ubiquitin conjugates by vacuolar proteases. The strains also carried pP_{CUP1}-*myc-UBI* to maintain a pool of free ubiquitin and to provide an epitope tag for detection of ubiquitin conjugates. After Gap1p-HA immunoprecipitation with rat anti-HA, samples were resolved by SDS-PAGE and immunoblotted with either mouse anti-HA (to detect Gap1p-HA) or mouse anti-*myc* (to detect conjugates with *myc*-tagged ubiquitin). Control immunoblots revealed significantly higher amount of polyubiquitinated species of Gap1p-HA in a *doa4*Δ *pep4*Δ P_{ADH1}-*GAP1-HA* strain (lane 4, in Figure 12A) than in a *pep4*Δ P_{ADH1}-*GAP1-HA* strain (lane 3). Samples run in parallel from identical strains expressing untagged endogenous Gap1p demonstrate that only Gap1p-HA was immunoprecipitated by the rat anti-HA (because no signal appears in lanes 1 and 2). This result confirmed a role of the Doa4p enzyme in the deubiquitination of Gap1p at the MVE. It appears that the deubiquitination of Gap1p before its entry into the MVE is carried out with the aim to recycle ubiquitin rather than being a prerequisite for the delivery of Gap1p into the MVE. Moreover, this genetic background, deficient in Gap1p deubiquitination, provides us with much more sensitive conditions for detecting variations in the accumulation of polyubiquitinated Gap1p under different conditions.

Neither lst4Δ *Nor Amino Acids Greatly Alter Gap1p Polyubiquitination*

We used this assay for the detection of ubiquitinated Gap1p to evaluate the extent to which Gap1p sorting to the vacuole during growth on glutamate or in an *lst4*Δ mutant might be a consequence of effects on Gap1p ubiquitination. We found

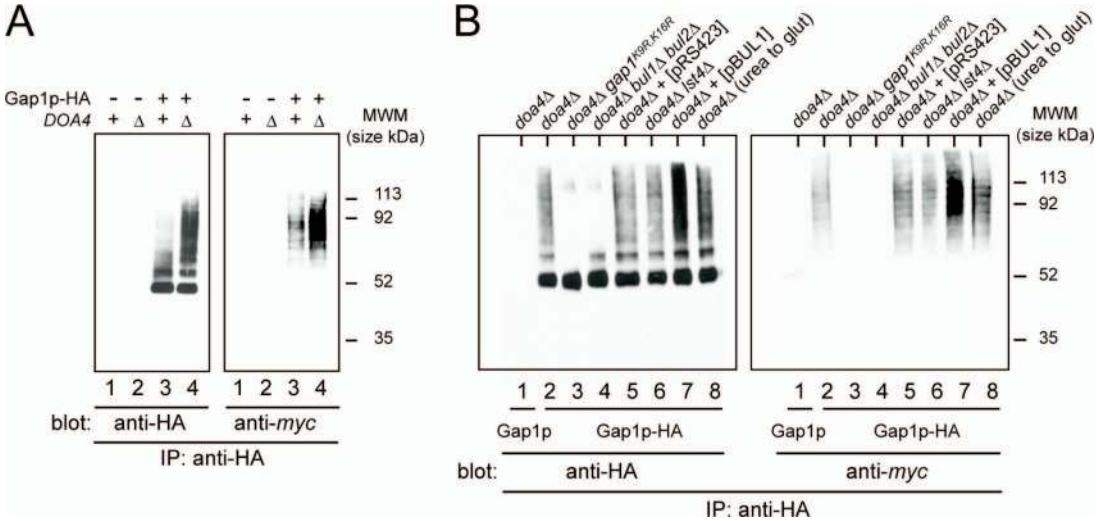

Figure 12. An *lst4*Δ mutation, as growth in glutamate, does not cause an increased accumulation in polyubiquitinated Gap1p comparable to the overproduction of Bul1p. (A) The polyubiquitinated state of Gap1p in the wild-type strain (lane 3, CKY868) versus a *doa4*Δ mutant (lane 4, CKY928) in a *pep4*Δ background expressing genomic P_{ADH1}-*GAP1-HA* and transformed with pP_{CUP1}-*myc-UBI*, was compared in immunoprecipitates from cells grown in minimal urea medium. Identical backgrounds (lane 1, CKY474, and lane 2, CKY993, respectively) expressing endogenous untagged Gap1p were utilized as negative controls. Immunoprecipitated samples were prepared as described in *Materials and Methods*, normalized, and 1/20 of the total loaded for SDS-PAGE and immunoblotting. Anti-HA (rat, 3F10) immunoprecipitates were immunoblotted with either anti-HA (16B12) mouse (left panel) or anti-*myc* (9E10) mouse (right panel). (B) Polyubiquitinated Gap1p-HA was isolated from *pep4*Δ P_{ADH1}-*GAP1-HA* strains containing the plasmid pP_{CUP1}-*myc-UBI* and 1/40 of the total normalized sample was loaded for SDS-PAGE and immunoblotted as in A. Samples from the strains analyzed are presented in the blots as follows: *doa4*Δ (lane 2, CKY928), *doa4*Δ *gap1*$^{K9R,\ K16R}$-*HA* (lane 3, CKY929), *doa4*Δ *bul1*Δ *bul2*Δ (lane 4, CKY930), *doa4*Δ *lst4*Δ (lane 6, CKY931), and *doa4*Δ (CKY1009) transformed with the empty plasmid pRS423 (lane 5), or the Bul1p overproducing strain pBUL1 (lane 7), and *doa4*Δ (CKY928) shifted for 1 h from urea to glutamate as the only nitrogen source (lane 8). A *doa4*Δ mutant strain expressing endogenous Gap1p served as a negative control (lane 1, CKY993).

previously that overexpression of *BUL1* or *BUL2* have a similar effect on targeting Gap1p to the vacuole as growth on glutamate or an *lst4*Δ mutant (Helliwell *et al.*, 2001). Thus, the possibility remains that amino acids or a null mutation in *LST4* could exert a positive effect on the Rsp5p/Bul1p/Bul2p ubiquitin ligase complex-dependent ubiquitination of Gap1p.

The amounts of ubiquitinated Gap1p-HA were compared in a genetic background with *doa4*Δ *pep4*Δ P_{ADH1}-*GAP1-HA* carrying the P_{CUP1}-*myc-UBI* plasmid. Strains carrying the mutations *bul1*Δ *bul2*Δ or an allele of *GAP1* with the two lysine acceptor sites for ubiquitination mutated to arginine (*gap1*^{K9R,K16R}; Soetens *et al.*, 2001) were used as negative controls to show that the dispersed high-molecular-weight species detected by Gap1p-HA immunoprecipitation followed by immunoblotting for *myc*-Ub in fact corresponded to polyubiquitinated Gap1p-HA (Figure 12A, and lanes 3 and 4 in Figure 12B). As a positive control to show the effect of hyperactivity of the Rsp5p/Bul1p/Bul2p ubiquitin ligase complex on Gap1p-HA ubiquitination, overexpression of Bul1p from a multicopy plasmid caused a corresponding increase in the amount of polyubiquitinated Gap1-HAp (Figure 12B, lane 7).

A *doa4*Δ *lst4*Δ mutant (lane 6) did not show increased levels of polyubiquitinated Gap1p-HA species when compared with a *doa4*Δ mutant alone (lane 2), showing that the effect of *lst4*Δ on Gap1p sorting is not an indirect consequence of hyper ubiquitination of Gap1p. When *doa4*Δ cells were transferred from urea medium to glutamate, only a modest increase in the amount of polyubiquitinated Gap1p-HA was observed (Figure 12B, lane 8). Although conditions of growth on glutamate medium cause Gap1p to be completely redirected from the plasma membrane to the vacuole, the corresponding increase in polyubiquitination of Gap1p-HA was much less than in the case of overexpression of *BUL1*. Thus a putative effect of glutamate on Gap1p ubiquitination does not suffice to explain the profound effect that amino acids have on Gap1p trafficking. Nevertheless we cannot yet rule out the possibility that intracellular amino acid concentrations exert, to some extent, their effect on Gap1p sorting by increasing the probability of Gap1p polyubiquitination.

DISCUSSION

Here we describe a comprehensive genome wide screen for genes required for the proper intracellular sorting of Gap1p in response to nitrogen source. Most of the mutations identified that increase the proportion of Gap1p sorted to the plasma membrane are in class E *VPS* genes that have been shown to be required for the formation of the MVE. These results establish that when Gap1p cannot enter the inwardly budding vesicles of the MVE efficient recycling of Gap1p from the endosome to the plasma membrane is possible. Genetic and physiological tests of the conditions under which cycling of Gap1p from endosome to the plasma membrane occurs show that high concentrations of amino acids can block cycling. Regulation of this cycling step appears to be the major physiological input of intracellular amino acid concentration in the overall process of regulating the amount of Gap1p delivered to the plasma membrane. The cycling step is also under genetic control by a collection of genes including *LST4* and *LST7*, and these genes are potential targets for regulation by amino acids.

A second stage of the intracellular sorting itinerary of Gap1p with the potential to be regulated by intracellular

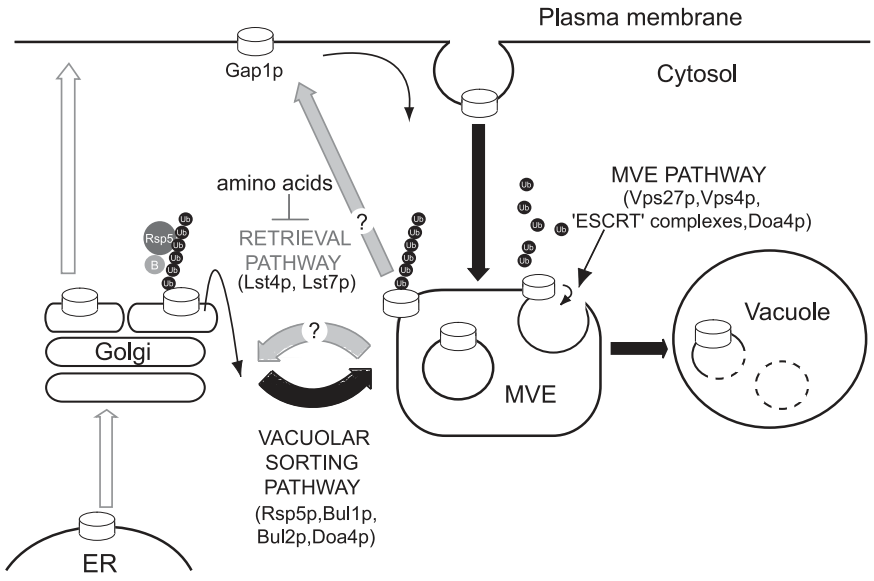

Figure 13. Proposed model for regulated Gap1p sorting in the endosome. Newly synthesized Gap1p has two possible fates once it reaches the *trans*-Golgi: sorting to the plasma membrane where it is active for amino acid uptake or to the vacuole for degradation. Polyubiquitination mediated by the Rsp5/Bul1p/Bul2p ubiquitin ligase complex is necessary for Gap1p delivery to the vacuolar sorting pathway (arrows in black). Polyubiquitinated Gap1p reaches the prevacuolar compartment where it has two possible fates: to become cargo for entry into multivesicular endosomes (MVE) or for recycling to the plasma membrane by a trafficking step that requires Lst4p and Lst7p (gray arrows). Recycling of Gap1p may occur by direct trafficking from the MVE to the plasma membrane or by way of the *trans*-Golgi. High intracellular concentrations of amino acids block Gap1p retrieval from the MVE. Before its delivery into the luminal vesicles of the MVE, Gap1p undergoes Doa4-dependent deubiquitination. By regenerating free ubiquitin, Doa4p also controls the rate of Rsp5/Bul1/Bul2-dependent polyubiquitination of newly synthesized Gap1p, earlier in the pathway. The MVE finally fuses to the vacuole, releasing the Gap1p-containing vesicles into the vacuolar lumen for degradation. Mutants that block formation of MVE vesicles (such as *vps4*Δ or *vps27*Δ) cause most Gap1p to follow the recycling pathway to the plasma membrane.

amino acids is ubiquitination of Gap1p, which enables Gap1p to be targeted to the endosome in the first place. The ubiquitination state of Gap1p is set by both ubiquitinating and deubiquitinating processes, and we developed an assay for the effect of intracellular amino concentration on the accumulation of ubiquitinated Gap1p based on the finding that deubiquitination of Gap1p could largely be eliminated by deletion of *DOA4*. In a *doa4*Δ genetic background a large fraction of the total Gap1p is in a polyubiquinated state, but the fraction of Gap1p that is ubiquitinated does not change significantly in the presence or absence of amino acids. Moreover, mutations such as *lst4*Δ, which have an effect on Gap1p sorting similar to growth in high amino acid concentrations, also does not give rise to a significant increase in the fraction of Gap1p that is polyubiquitinated. These results lead us to conclude that poyubiquitination of Gap1p alone does not suffice to explain the dramatic effect that amino acids exert in the down-regulation of Gap1p. Regulation of Gap1p recycling must constitute an additional and very likely more important target for the regulation of Gap1p sorting by amino acid levels.

Figure 13 outlines the two proposed decision points in Gap1p sorting in the late secretory pathway, showing the steps affected by intracellular amino acids and each of the different classes of mutants known to affect the distribution of Gap1p in the cell. The first decision appears to take place in the *trans*-Golgi and depends on Gap1p ubiquitination by the Rsp5p/Bul1p/Bul2p ubiquitin ligase complex (Helliwell *et al.*, 2001; Soetens *et al.*, 2001). The second sorting decision is made in the MVE, and at this stage Gap1p can either be recycled to the plasma membrane by an *LST4*-dependent process or can be sorted into endosomal vesicles by ESCRT complex proteins.

We cannot, nor do we wish to, rule out the possibility that Gap1p recycling to the plasma membrane occurs by a direct MVE to plasma membrane transport step, as has been indicated for trafficking of misfolded Pma1p (Luo and Chang, 2000). However, when the partitioning probabilities for sorting decisions in both the Golgi and MVE are considered, we believe the present data indicates that Gap1p normally cycles between the TGN and MVE compartments. In the presence of high intracellular amino acid concentrations (or in an *lst4*Δ mutant) the amount of Gap1p delivered to the plasma membrane is only a few percent of the amount delivered in an ubiquitination defective mutant such as *bul1*Δ *bul2*Δ. This result shows that in a wild-type cell most Gap1p is initially transported to the MVE compartment where the amino acid–dependent sorting decision takes place. In the absence of high intracellular amino acids (or in a subset of ESCRT mutants) Gap1p is efficiently cycled from the MVE to the plasma membrane. Importantly, when either Bul1p or Bul2p is overproduced, most of Gap1p can be returned to the VPS pathway, showing that Gap1p that is recycled from the MVE enters a compartment that can still be influenced by the rate of Bul-dependent ubiquitination. This Bul-dependent compartment is most likely the TGN and not the plasma membrane because endocytosis defective mutants have little effect on the amount of Gap1p partitioned to the plasma membrane. It appears that Gap1p may cycle between the TGN and MVE multiple times—the sorting probabilities in each of these compartments thus determining the overall partitioning of Gap1p between the plasma membrane and vacuole.

In agreement with our observations, Bugnicourt *et al.* (2004) have recently shown that ESCRT mutants cause recycling of the uracil permease, Fur4p, to the cell surface. In this case, they observed a block in Fur4p recycling in double mutants simultaneously affecting components of the ESCRT and HOPS complexes (the latter is involved in vacuolar fusion events; see Wickner, 2002). These observations were interpreted to indicate that Fur4p recycling is mediated by the HOPS-dependent pathway, which bypasses the Golgi. Similarly, Nikko *et al.* (2003) observed that in *S. cerevisiae* cells of the Σ1278b genetic background the cell surface accumulation of Gap1p in a *bro1*Δ mutant in the presence of ammonia is abolished by a simultaneous mutation in *VAM3* or *VAM7* genes, also suggesting the possible existence of a recycling pathway from the vacuolar and/or late endosomal membranes to the cell surface independent from the Golgi. Although we do not rule out that such a pathway may also

exist for Gap1p, in our genetic background (S288C) we found that *vam3*Δ or *vam7*Δ mutations have no significant effect on Gap1p sorting (as shown in Tables 3 and 4, and Figure 7). We find that null mutations in genes encoding for components of the HOPS complex (such as *vps16*Δ or *pep3*Δ) caused significantly elevated levels of Gap1p activity rather than decreased levels that would be predicted if the HOPS complex were required for cycling of Gap1p to the plasma membrane. Moreover, these mutations did not have a significant effect on cycling of Gap1p to the plasma membrane in the presence of the class E vps mutation *vps4*Δ. These results indicate that mutations in the HOPS complex may have a similar effect on Gap1p trafficking as ESCRT mutants that block progression of Gap1p from the MVE to the vacuole.

In contrast, mutations such as *lst4*Δ and *lst7*Δ, which block Gap1p recycling to the plasma membrane, cause a dramatic reduction in Gap1p activity in cells grown on medium without amino acids. This simple assay has allowed us to test other mutants known to participate in endosome to Golgi trafficking for a specific effect on Gap1p recycling. As shown in Tables 3 and 4 and in Figure 7, we did not detect a significant effect on Gap1p activity by mutations in the retrograde complex or in retromer components. These mutations did not interfere with the efficient cycling of Gap1p to the plasma membrane in the presence of an ESCRT mutation such as *vps4*Δ.

Interestingly, although mutations such as *lst4*Δ and *lst7*Δ have a profound effect on Gap1p activity, this and other mutations identified in the screen that block Gap1p cycling to the cell surface do not seem to cause a more generalized defect on trafficking as shown by the normal CPY sorting and FM4-64 recycling patterns in the corresponding null mutant strains (Figure 8; and Gao and Kaiser, unpublished results). Taken together, the specificity of these different classes of cycling mutants for different cargo proteins implies the existence of at least two genetically distinct pathways for endosome-to-Golgi trafficking.

A recent report revealed a possible role of GGA proteins in facilitating transport of Gap1p from the TGN to a prevacuolar compartment (Scott *et al.*, 2004). Although a possible role of these proteins in increasing the efficiency of Gap1p vacuolar sorting rate may exist, Gap1p sorting to the VPS pathway does not absolutely depend on these functions because an *lst4*Δ *gga1*Δ *gga2*Δ double mutant still shows constitutive sorting of Gap1p to the vacuole. Data shown by Scott *et al.* (2004) indicated that the defect in vacuolar sorting observed in a *gga1*Δ *gga2*Δ double mutant is only partial and that it may be related to defective endocytic trafficking. Because here we show that *LST4* must have a role in Gap1p sorting that is independent from endocytosis of the permease, it is therefore possible that GGA-dependent sorting of Gap1p occurs only in specific steps of the vacuolar sorting of Gap1p (e.g., in the formation of endocytic vesicles).

Several recent studies have indicated a direct action of Rsp5p on different cargo at the MVE (Blondel *et al.*, 2004; Dunn *et al.*, 2004; Katzmann *et al.*, 2004; Morvan *et al.*, 2004). In all of these cases the corresponding cargo proteins accumulate at the MVE in an *rsp5*-deficient background. By contrast, mutations affecting the polyubiquitinating machinery Rsp5p/Bul1p/Bul2p cause Gap1p to be localized at the cell surface, not the MVE. Most importantly in a *bul1*Δ *bul2*Δ double mutant either the presence of high intracellular amino acids or a *lst4*Δ mutation have no effect on the trafficking of Gap1p to the cell surface, indicating that in the absence of ubiquitination Gap1p never reaches the sorting step controlled by amino acids and Lst4p. The most straightforward explanation for this result is that amino acids and Lst4p control sorting at the membrane of the MVE and that the sorting step governed by Rsp5/Bul1/Bul2p action on Gap1p takes place at an earlier stage of the pathway, most likely in the *trans*-Golgi.

Although sharing similar features in their vacuolar sorting through the MVE pathway, other permeases have already shown differences with Gap1p in the particular steps governing their ubiquitination. For instance, although Rsp5p plays an important role in Fur4p MVE sorting, the polyubiquitination of the uracil permease does not seem to depend on Bul proteins (Blondel *et al.*, 2004).

The availability of Gap1p for its own recycling out of the MVE may be the result of a balance between the state of Gap1p polyubiquitination, its consequent recognition by ESCRT proteins, and the state activity status of both Lst4p and the components of the recycling sorting machinery for Gap1p in response to amino acid concentrations. Such regulation could determine the ability of any putative recycling machinery to compete for Gap1p interaction, with certain ESCRT machinery components specialized for recognition of Gap1p as MVE cargo. In this regard, our results show that different subsets of ESCRT proteins may have a more important role than others in the ability to retain Gap1p for its MVE sorting. Our results provide additional evidence that ESCRT proteins have differential roles in the sorting of specific MVE cargo, as suggested by previous works (Kranz *et al.*, 2001; Köhler, 2003).

In agreement with previous observations made by Nikko *et al.* (2003) in our experimental conditions a *bro1*Δ mutant showed higher Gap1p activity than the rest of ESCRT mutations, reaching levels comparable to those displayed by mutations in the polyubiquitinating machinery or *DOA4*. Although the combination with an *lst4*Δ mutation rescued the ability of a *bro1*Δ mutant to grow in the presence of low levels of ADCB by reducing Gap1p activity, this double mutant exhibited an unusually high percentage of Gap1p-GFP located at the cell surface. The similarity of *doa4*Δ and *bro1*Δ mutations on their effect on Gap1p sorting can now be explained by the recent discovery that Bro1p functions to recruitment of Doa4p to endosomal membranes (Luhtala and Odorizzi, 2004).

Future analysis involving further characterization of the amino acids ability to modulate the activities of the steps controlled by Rsp5/Bul1/Bul2p, ESCRT proteins, Lst4p, Lst7p, and recycling machinery will help to elucidate how metabolic signals can change the final fate of Gap1p and other plasma membrane proteins.

ACKNOWLEDGMENTS

We thank Barbara Karampalas and Hongjing Qu for technical assistance and members of the Kaiser lab for materials and advice. We also thank Dr. Susan L. Lindquist for her generosity and patient support during the latest stages of this work. This work was supported by a National Institute of General Medical Sciences Grant GM56933 to C.A.K.

REFERENCES

Adams, A., Gottschling, D., and Kaiser, C. (1996). Methods in Yeast Genetics: A Laboratory Course Manual, New York: Cold Spring Harbor Laboratory Press.

Amerik, A. Y., Nowak, J., Swaminathan, S., and Hochstrasser, M. (2000). The Doa4 deubiquitinating enzyme is functionally linked to the vacuolar protein-sorting and endocytic pathways. Mol. Biol. Cell *11*, 3365–3380.

Babst, M. (2005). A protein's final ESCRT. Traffic *6*, 2–9.

Babst, M., Katzmann, D. J., Estepa-Sabal, E. J., Meerloo, T., and Emr, S. D. (2002a). ESCRT-III: an endosome-associated heterooligomeric protein complex required for MVB sorting. Dev. Cell *3*, 271–282.

Babst, M., Katzmann, D. J., Snyder, W. B., Wendland, B., and Emr, S. D. (2002b). Endosome-associated complex, ESCRT-II, recruits transport machinery for protein sorting at the multivesicular body. Dev. Cell *3*, 283–289.

Babst, M., Odorizzi, G., Estepa, E. J., and Emr, S. D. (2000). Mammalian tumor susceptibility gene 101 (*TSG101*) and the yeast homologue, Vps23p, both function in late endosomal trafficking. Traffic *1*, 248–258.

Babst, M., Wendland, B., Estepa, E. J., and Emr, S. D. (1998). The Vps4p AAA ATPase regulates membrane association of a Vps protein complex required for normal endosome function. EMBO J. *17*, 2982–2993.

Becherer, K. A., Rieder, S. E., Emr, S. D., and Jones, E. W. (1996). Novel syntaxin homologue, Pep12p, required for the sorting of lumenal hydrolases to the lysosome-like vacuole in yeast. Mol. Biol. Cell *7*, 579–594.

Benedetti, H., Raths, S., Crausaz, F., and Riezman, H. (1994). The *END3* gene encodes a protein that is required for the internalization step of endocytosis and for actin cytoskeleton organization in yeast. Mol. Biol. Cell *5*, 1023–1037.

Bilodeau, P. S., Winistorfer, S. C., Kearney, W. R., Robertson, A. D., and Piper, R. C. (2003). Vps27-Hse1 and ESCRT-I complexes cooperate to increase efficiency of sorting ubiquitinated proteins at the endosome. J. Cell Biol. *163*, 237–243.

Bilodeau, P. S., Winistorfer, S. C., Allaman, M. M., Surendhran, K., Kearney, W. R., Robertson, A. D., and Piper, R. C. (2004). The GAT domains of clathrin-associated GGA proteins have two ubiquitin binding motifs. J. Biol. Chem. *279*, 54808–54816.

Blondel, M. O., Morvan, J., Dupré, S., Urban-Grimal, D., Haguenauer-Tsapis, R., and Volland, C. (2004). Direct sorting of the yeast uracil permease to the endosomal system is controlled by uracil binding and Rsp5-dependent ubiquitylation. Mol. Biol. Cell *15*, 883–895.

Bonifacino, J. S. (2004). The GGA proteins: adaptors on the move. Nat. Rev. Mol. Cell. Biol. *5*, 23–32.

Brachmann, C. B., Davies, A., Cost, G. J., Caputo, E., Li, J., Hieter, P., and Boeke, J. D. (1998). Designer deletion strains derived from *Saccharomyces cerevisiae* S288C: a useful set of strains and plasmids for PCR-mediated gene disruption and other applications. Yeast *14*, 115–132.

Bugnicourt, A., Froissard, M., Sereti, K., Ulrich, H. D., Haguenauer-Tsapis, R., and Galan, J. M. (2004). Antagonistic roles of ESCRT and Vps class C/HOPS complexes in the recycling of yeast membrane proteins. Mol. Biol. Cell *15*, 4203–4214.

Butow, R. A., and Avadhani, N. G. (2004). Mitochondrial signaling: the retrograde response. Mol. Cell *14*, 1–15.

Chen, E. J., and Kaiser, C. A. (2003). LST8 negatively regulates amino acid biosynthesis as a component of the TOR pathway. J. Cell Biol. *161*, 333–347.

Chen, E. J., and Kaiser, C. A. (2002). Amino acids regulate the intracellular trafficking of the general amino acid permease of *Saccharomyces cerevisiae*. Proc. Natl. Acad. Sci. USA *99*, 14837–14842.

Christianson, T. W., Sikorski, R. S., Dante, M., Shero, J. H., and Hieter, P. (1992). Multifunctional yeast high-copy number shuttle vectors. Gene *110*, 119–122.

Conibear, E., and Stevens, T. H. (2000). Vps52p, Vps53p, and Vps54p form a novel multisubunit complex required for protein sorting at the yeast late Golgi. Mol. Biol. Cell *11*, 305–323.

Courchesne, W. E., and Magasanik, B. (1983). Ammonia regulation of amino acid permeases in *Saccharomyces cerevisiae*. Mol. Cell. Biol. *3*, 672–683.

Dunn, R., Klos, D. A., Adler, A. S., and Hicke, L. (2004). The C2 domain of the Rsp5 ubiquitin ligase binds membrane phosphoinositides and directs ubiquitination of endosomal cargo. J. Cell Biol. *165*, 135–144.

Dupré, S., and Haguenauer-Tsapis, R. (2001). Deubiquitination step in the endocytic pathway of yeast plasma membrane proteins: crucial role of Doa4p ubiquitin isopeptidase. Mol. Cell Biol. *21*, 4482–4494.

Ecker, D. J., Khan, M. I., Marsh, J., Butt, T. R., and Crooke, S. T. (1987). Chemical synthesis and expression of a cassette adapted ubiquitin gene. J. Biol. Chem. *262*, 3524–3527.

Ellison, M. J., and Hochstrasser, M. (1991). Epitope-tagged ubiquitin. A new probe for analyzing ubiquitin function. J. Biol. Chem. *266*, 21150–21157.

Goldstein, A. L., and McCusker, J. H. (1999). Three new dominant drug resistance cassettes for gene disruption in *Saccharomyces cerevisiae*. Yeast *15*, 1541–1553.

Grenson, M., Hou, C., and Crabeel, M. (1970). Multiplicity of the amino acid permeases in *Saccharomyces cerevisiae*. IV. Evidence for a general amino acid permease. J. Bacteriol. *103*, 770–777.

Helliwell, S. B., Losko, S., and Kaiser, C. A. (2001). Components of a ubiquitin ligase complex specify polyubiquitination and intracellular trafficking of the general amino acid permease. J. Cell Biol. *153*, 649–662.

Hicke, L. (1997). Ubiquitin-dependent internalization and down-regulation of plasma membrane proteins. FASEB J. *11*, 1215–1226.

Horák, J. (2003). The role of ubiquitin in down-regulation and intracellular sorting of membrane proteins: insights from yeast. Biochim. Biophys. Acta *1614*, 139–155.

Jauniaux, J. C., and Grenson, M. (1990). GAP1, the general amino acid permease gene of *Saccharomyces cerevisiae*. Nucleotide sequence, protein similarity with the other bakers yeast amino acid permeases, and nitrogen catabolite repression. Eur. J. Biochem. *190*, 39–44.

Katzmann, D. J., Sarkar, S., Chu, T., Audhya, A., and Emr, S. D. (2004). Multivesicular body sorting: ubiquitin ligase Rsp5 is required for the modification and sorting of carboxypeptidase S. Mol. Biol. Cell *15*, 468–480.

Katzmann, D. J., Stefan, C. J., Babst, M., and Emr, S. D. (2003). Vps27 recruits ESCRT machinery to endosomes during MVB sorting. J. Cell Biol. *160*, 413–423.

Katzmann, D. J., Odorizzi, G., and Emr, S. D. (2002). Receptor downregulation and multivesicular body sorting. Nat. Rev. Mol. Cell Biol. *3*, 893–905.

Katzmann, D. J., Babst, M., and Emr, S. D. (2001). Ubiquitin-dependent sorting into the multivesicular body pathway requires the function of a conserved endosomal protein sorting complex, ESCRT-I. Cell *106*, 145–155.

Köhler, J. R. (2003). Mos10 (Vps60) is required for normal filament maturation in *Saccharomyces cerevisiae*. Mol. Microbiol. *49*, 1267–1285.

Kranz, A., Kinner, A., and Kölling, R. (2001). A family of small coiled-coil-forming proteins functioning at the late endosome in yeast. Mol. Biol. Cell *12*, 711–723.

Laney, J. D., and Hochstrasser, M. (2002). Assaying protein ubiquitination in *Saccharomyces cerevisiae*. Methods Enzymol. *351*, 248–257.

Lafourcade, C., Galan, J. M., Gloor, Y., Haguenauer-Tsapis, R., and Peter, M. (2004). The GTPase-activating enzyme Gyp1p is required for recycling of internalized membrane material by inactivation of the Rab/Ypt GTPase Ypt1p. Mol. Cell. Biol. *24*, 3815–3826.

Longtine, M. S., McKenzie, A., Demarini, D. J., Shah, N. G., Wach, A., Brachat, A., Philippsen, P., and Pringle, J. R. (1998). Additional modules for versatile and economical PCR-based gene deletion and modification in *Saccharomyces cerevisiae*. Yeast *14*, 953–961.

Luhtala, N., and Odorizzi, G. (2004). Bro1 coordinates deubiquitination in the multivesicular body pathway by recruiting Doa4 to endosomes. J. Cell Biol. *166*, 717–729.

Luo, W., and Chang, A. (2000). An endosome-to-plasma membrane pathway involved in trafficking of a mutant plasma membrane ATPase in yeast. Mol. Biol. Cell *11*, 579–592.

Magasanik, B., and Kaiser, C. A. (2002). Nitrogen regulation in *Saccharomyces cerevisiae*. Gene *290*, 1–18.

Morvan, J., Froissard, M., Haguenauer-Tsapis, R., and Urban-Grimal, D. (2004). The ubiquitin ligase Rsp5p is required for modification and sorting of membrane proteins into multivesicular bodies. Traffic *5*, 383–392.

Nikko, E., Marini, A. M., and André, B. (2003). Permease recycling and ubiquitination status reveal a particular role for Bro1 in the multivesicular body pathway. J. Biol. Chem. *278*, 50732–50743.

Odorizzi, G., Katzmann, D. J., Babst, M., Audhya, A., and Emr, S. D. (2003). Bro1 is an endosome-associated protein that functions in the MVB pathway in *Saccharomyces cerevisiae*. J. Cell Sci. *116*, 1893–1903.

Pizzirusso, M., and Chang, A. (2004). Ubiquitin-mediated targeting of a mutant plasma membrane ATPase, Pma1-7, to the endosomal/vacuolar system in yeast. Mol. Biol. Cell *15*, 2401–2409.

Raiborg, C., Rusten, T. E., and Stenmark, H. (2003). Protein sorting into multivesicular endosomes. Curr. Opin. Cell Biol. *15*, 446–455.

Raymond, C. K., Howald-Stevenson, I., Vater, C. A., and Stevens, T. H. (1992). Morphological classification of the yeast vacuolar protein sorting mutants: evidence for a prevacuolar compartment in class E *vps* mutants. Mol. Biol. Cell *3*, 1389–1402.

Reddy, J. V., and Seaman, M. N. (2001). Vps26p, a component of retromer, directs the interactions of Vps35 in endosome-to-Golgi retrieval. Mol. Biol. Cell *12*, 3242–3256.

Reggiori, F., and Pelham, H. R. (2001). Sorting of proteins into multivesicular bodies: ubiquitin-dependent and -independent targeting. EMBO J. *20*, 5176–5186.

Roberg, K. J., Rowley, N., and Kaiser, C. A. (1997a). Physiological regulation of membrane protein sorting late in the secretory pathway of *Saccharomyces cerevisiae*. J. Cell Biol. *137*, 1469–1482.

Roberg, K. J., Bickel, S., Rowley, N., and Kaiser, C. A. (1997b). Control of amino acid permease sorting in the late secretory pathway of *Saccharomyces cerevisiae* by *SEC13*, LST4, LST7, and LST8. Genetics *147*, 1569–1584.

Sambrook, J., Fritsch, E. F., and Maniatis, T. (1997). Molecular Cloning: A Laboratory Manual, 2nd ed., ed. C. Nolan, Cold Spring Harbor, NY: Cold Spring Harbor Laboratory Press.

Scott, P. M., Bilodeau, P. S., Zhdankina, O., Winistorfer, S. C., Hauglund, M. J., Allaman, M. M., Kearney, W. R., Robertson, A. D., Boman, A. L., and Piper, R. C. (2004). GGA proteins bind ubiquitin to facilitate sorting at the trans-Golgi network. Nat. Cell Biol. *6*, 252–259.

Seaman, M. N. (2005). Recycle your receptors with retromer. Trends Cell Biol. *15*, 68–75.

Sikorski, R. S., and Hieter, P. (1989). A system of vectors and yeast host strains designed for efficient manipulation of DNA in *Saccharomyces cerevisiae.* Genetics *122*, 19–27.

Siniossoglou, S., and Pelham, H. R. (2002). Vps51p links the VFT complex to the SNARE Tlg1p. J. Biol. Chem. *277*, 48318–483324.

Soetens, O., De Craene, J. O., and André, B. (2001). Ubiquitin is required for sorting to the vacuole of the yeast general amino acid permease, Gap1. J. Biol. Chem. *276*, 43949–43957.

Springael, J. Y., Galan, J. M., Haguenauer-Tsapis, R., and André, B. (1999). NH4+-induced down-regulation of the *Saccharomyces cerevisiae* Gap1p permease involves its ubiquitination with lysine-63-lynked chains. J. Cell Sci. *112*, 1375–1383.

Stanbrough, M., and Magasanik, B. (1995). Transcriptional and posttranslational regulation of the general amino acid permease of *Saccharomyces cerevisiae.* J. Bacteriol. *177*, 94–102.

Swaminathan, S., Amerik, A. Y., and Hochstrasser, M. (1999). The Doa4 deubiquitinating enzyme is required for ubiquitin homeostasis in yeast. Mol. Biol. Cell *10*, 2583–2594.

Urbanowski, J., and Piper, R. C. (1999). The iron transporter Fth1p forms a complex with the Fet5 iron oxidase and resides on the vacuolar membrane. J. Biol. Chem. *274*, 38061–38070.

Vandenbol, M., Jauniaux, J. C., and Grenson, M. (1989). Nucleotide sequence of the *Saccharomyces cerevisiae PUT4* proline-permease-encoding gene: similarities between CAN1, HIP1 and PUT4 permeases. Gene *83*, 153–159.

Vida, T. A., and Emr, S. D. (1995). A new vital stain for visualizing vacuolar membrane dynamics and endocytosis in yeast. J. Cell Biol. *128*, 779–792.

Whyte, J. R., and Munro, S. (2002). Vesicle tethering complexes in membrane traffic. J. Cell Sci. *115*, 2627–2637.

Wickner, W. (2002). Yeast vacuoles and membrane fusion pathways. EMBO J. *21*, 1241–1247.

Wiederkehr, A., Avaro, S., Prescianotto-Baschong, C., Haguenauer-Tsapis, R., and Riezman, H. (2000). The F-box protein Rcy1p is involved in endocytic membrane traffic and recycling out of an early endosome in *Saccharomyces cerevisiae.* J. Cell Biol. *149*, 397–410.